Reviewer #1

The authors aim to investigate the complicated impacts of synoptic forcing and aerosol radiative effect on boundary layer and pollution in the Beijing-Tianjin-Hebei region of China. The manuscript has well-presented some findings. However, there are still some minor concerns that need to be addressed.

Thanks for taking time to review our manuscript and offer helpful suggestions! We carefully revised the manuscript, please see the response below.

1. Most of all, more deeper analyses are needed for all of the figures. In the current version, the analysis is too simple and rough for the figures. Besides, a mechanism analysis should be performed according to the phenomena.

More analyses and discussions were added for most figures as suggested. For the associations between synoptic pattern and PBL structure, more meteorological parameters (e.g., temperature and relatively humidity) were compared and analyzed. In addition to the synoptic Type 2, the impacts of Type 4 on PBL and aerosol pollution were also elucidated based on the long-term soundings and $PM_{2.5}$ measurements.

Besides, instead analyzing those two episodes roughly, in the revised manuscript we focused on the pollution episode at the end of December 2017 and tried our best to unravel the links among the evolution of synoptic conditions (i.e., Type 4 on December 27, Type 2 on December 28-29, Type 1 on December 30-31), PBL structure, aerosol vertical distribution, as well as the aerosol radiative effect. The possible mechanisms related to the development of PBL were carefully given based on the abovementioned observational and simulated analysis.

2. In the Abstract section, Line 10-15, the meaning of "To unravel the complicated impacts of large-scale atmospheric forcing and the local-scale planetary boundary layer (PBL) characteristics on the pollution there" is unclear. Moreover, the title illustrated that the focus of this study is the "impacts of synoptic forcing and aerosol radiative effect on boundary layer and pollution". The Abstract needs more improvements.

The sentence mentioned were rewritten as:

"The heavy aerosol pollutions frequently occur in winter, closely in relation to the planetary boundary layer (PBL) meteorology. To unravel the physical processes that influence the PBL structure and aerosol pollution in BTH, this study combined long-term observational data analyses, synoptic pattern classification, and meteorology-chemistry coupled simulations."

Since more analyses were added, most of the abstract were re-written and highlighted the integrated impacts of synoptic pattern and aerosol radiative effect.

3. What is the standard to identify the heavy pollution episodes in Figure 2?

The heavy pollution episode was identified when the maximum daily $PM_{2.5}$ concentration is greater than 100 μg m^{-3} in both Beijing and Tangshan. The relevant information was added in the figure title.

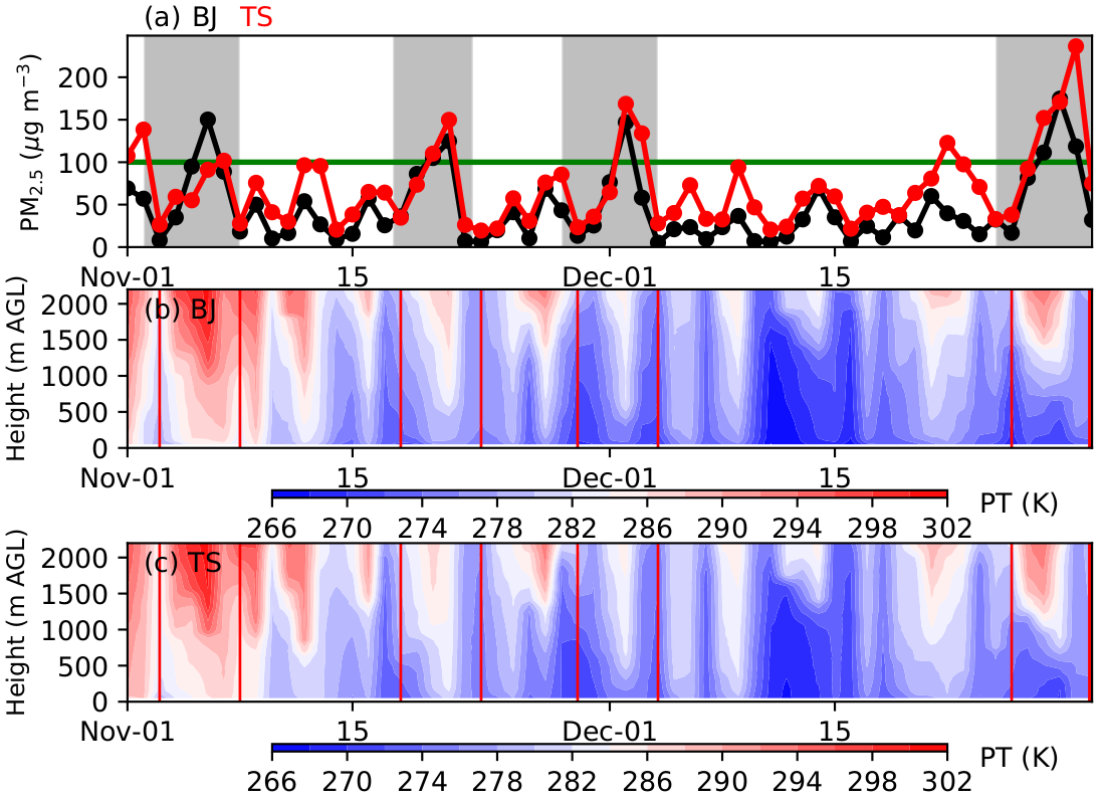

Fig. 2. Time series of observed $PM_{2.5}$ concentration from 1 November to 31 December in 2017 in (a) Beijing and Tangshan, and (b, c) vertical structure of potential temperature (PT) derived from the sounding data at 2000 BJT. Four heavy pollution episodes with maximum daily $PM_{2.5}$ concentration greater than 100 μg m^{-3} in both

Beijing and Tangshan are marked by the grey shadings in Fig. 2a.

4. The abbreviation should be used in the following illustration after definition.

Thanks for your kind suggestion. The definitions of abbreviation were added in revised manuscript, and some abbreviations were removed (e.g., ROI).

5. Section 2 should be separated the two parts including "Data" and "model description".

The Section 2 was separated as suggested.

6. In Figure 6, the legend should be given in (a).

Revised as suggested.

7. Figure 7-9, are these results the model simulation or reanalysis results? It should be present clearly in figure title.

All these figures presented the model simulations. The information was clearly stated in the figure titles as suggested.

8. The black line in Figure 7 is not clear.

In the revised manuscript, we reorganized the manuscript and removed the Figure 7.

9. In Figure 8-9, what is the meaning of gray color shading? In Figure 10a and 10b, what does the white color denote?

The grey color shadings in Figs. 8-9 denote the mountains. In Fig. 10a and 10b, the white color shadings also denotes the mountains. In the revised manuscript, all the mountains were denoted by the grey shadings and clearly stated in the figure titles.

10. Page 5, Line 151, the sentence "As the estimated BLH shown in Fig. 5" need to be rephrased.

In the revised manuscript, the sentence was revised as: "Fig. 5 shows the time series of simulated BLH in Beijing and Tangshan."

11. What is the meaning of “region of interest”? Some abbreviation is not needed. For example, ROI.

The “region of interest” is the region we primarily focused on. To be clear, in the revised manuscript, the abbreviation was removed as suggested.

Reviewer #2

This work tried to understand integrated impacts of synoptic forcing and aerosol radiative effect on boundary layer and pollution in the BTH region based on weather typing as well as chemistry-meteorology coupled regional model. I think it is an interesting topic of great importance. By combining observed data together with simulations, the author analyzed the impact of different synoptic patterns and aerosol radiative effect on heavy haze pollution in BTH. The influence of the primary synoptic type and aerosols' feedback are displayed very well separately, while the joint effect of these two processes are not very clear. For example, which synoptic type is more conducive for the feedback formation and why? Are the differences of pollution level under different synoptic patterns due primarily to regional circulation or intensity of aerosol radiative impact and even more secondary aerosol formation? Overall, more in-depth analysis ought to be provided. Here are some issues that need to be addressed for further improving this work.

Thanks for reviewing our manuscript and giving constructive suggestions to improve our manuscript! We have carefully revised the manuscript, and tried our best to analyze the joint effect during the aerosol pollution in BTH. Instead of analyzing those two episodes roughly, in the revised manuscript we focused on the pollution episode at the end of December 2017 and tried to unravel the links among the evolution of synoptic conditions, PBL structure, aerosol vertical distribution, as well as the aerosol radiative effect. It's found the Type 2 is more conducive for the feedback than Type 4, since more aerosols can be transported to the upper levels (Wang et al., 2018).

In the revised manuscript, the simulations with/without the aerosol radiative effect were compared. Although the aerosol radiative effect can modulate the pollution level, the general variations of aerosol concentration were governed by the evolution of synoptic weather. For the secondary aerosol formation, it is also relevant to the occurrence of certain stagnant synoptic conditions. The variation of the synoptic patterns modulated the ambient pollutants and likely provided the primary driving force for the day-to-day variations in air pollution level (e.g., Chen et al., 2008; Wei et al., 2011; Zhang et al., 2012; Hu et al., 2014; Zhang et al., 2016; Ye et al., 2016; Miao et al., 2017).

Major comments:

1. This study used T-PCA method to identify main synoptic weather in Section 3.1. I wonder if the sample size is too small to get the representative results. Usually, years of GPH data was utilized for weather classification (Zhang et al., 2016). Another, the domain of used FNL data is not very clear. Did the author just use the FNL data in BTH region as shown in Fig. 3? Can this region well capture the various spatial-scale circulation systems, especially large-scale ones? At last, it seems that Type 4 is more polluted than Type 2 and occurred during 28-31 Dec. in the following case discussed in 3.2, why the synoptic type 2 can be regarded as the representative polluted pattern (Line 133-135)?

In the synoptic classification, the domain of FNL data used was centered the BTH and covered an area of 106-126 °E in longitude and 29-49 °N in latitude, which was also the domain of WRF-Chem simulation (Fig. 1a). Unlike the previous work of Zhang et al. (2016) that investigated the linkage between East Asian Monsoon, synoptic weather, and air quality in the North China Plain from 1980 to 2013, this study focused on the day-to-day variation of wintertime synoptic condition in BTH during 2017 and 2018. Although both applied weather typing techniques, Zhang et al. (2016) focused on the inter-annual/decadal variability of monsoon, while we focused on the day-to-day evolution of mid-latitude systems in winter. Thus, a relatively smaller domain of interest was used in this study. By examining the simulated GH fields during the selected pollution episode, it's found that the day-to-day evolutions of mid-latitude systems that influence the BTH can be well captured in the domain of interest. In the revised manuscript, the previous work of Zhang et al. (2016) was cited in the Introduction to support the important roles of synoptic weather in air pollution.

To address the concern about data length (8 months, 240 days), we have tested the synoptic classification by extending the data to 24 months (winter months from 2013 to 2018, 721 days). As shown below, similar patterns (Types 1, 2, and 4) were identified. Since we primarily analyzed the PBL structure and pollution levels under these patterns, the sample size cannot affect the main findings in this study. The 8-month data were long enough to identify the typical patterns associated with the heavy pollution in winter

(Types 2 and 4).

For the representative polluted pattern, we not only considered the pollution level but also the occurrence frequency. Therefore, the Type 2 is regarded as the representative pattern. We agreed with the reviewer that the Type 4 is another important pattern associated with the heavy pollution in BTH, despite of its low occurrence frequency (~5 %). In the revised manuscript, the influences of Type 4 on PBL structure and aerosol transport during the selected episode were analyzed and compared with those of Type 2.

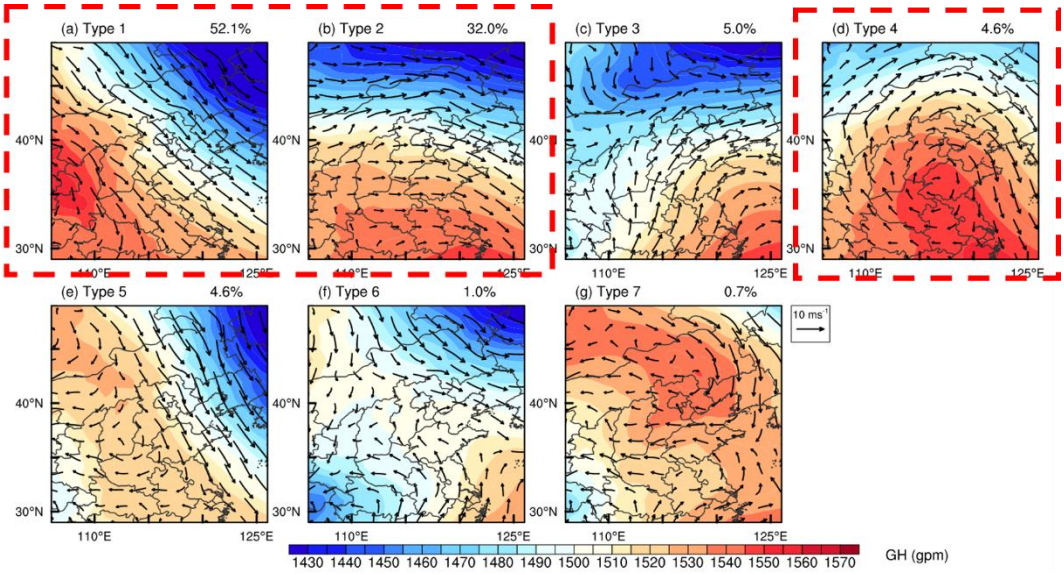

Fig. R1. The 850-hPa geopotential height (GH) fields and wind vectors for the seven classified patterns, identified using the T-PCA method and wintertime reanalysis data from 2013 to 2018. The frequency of each synoptic pattern is also given.

2. One strength of this work is comprehensive observational data. Here, modeled meteorological conditions like air temperature wind speed and RH was validated in detail. However, the modeled air pollution, especially aerosol reproduction, ought to be evaluated since that this work mainly focused on aerosols' impact on meteorology. Thus, the WRF-Chem simulation with/without aerosol radiative effects is suggested to be compared with observed temperature, RH and hourly $PM_{2.5}$ concentration.

Thanks for you kind suggestion! In the revised manuscript, more observations (e.g., 1000-m air temperature and 200-m relative humidity) were added to characterize the

PBL of different synoptic types (Fig. 4). Among those seven identified synoptic patterns, Types 2 and 4 are associated with heavier pollution level. Both types are characterized by stronger thermal stability (Fig. 4b), warmer upper air (Fig. 4c), and higher near-surface relative humidity (Fig. 4d).

For the validation of WRF-Chem model, the simulations with/without aerosol radiative effect were compared with the observed temperature, relative humidity (RH), and $PM_{2.5}$ concentration in Beijing and Tangshan (Fig. 6). The variations of temperature, RH and $PM_{2.5}$ concentration can be generally well reproduced by the model, although discrepancies existed. Comparing the simulations with aerosol radiative effect (BASE) to those without (EXP), the BASE has slightly higher $PM_{2.5}$ concentrations, higher RHs and lower temperatures, which lead to higher correlation coefficients with observations. In the revised manuscript, the relevant analyses were added in the Sections 3.1 and 3.2.

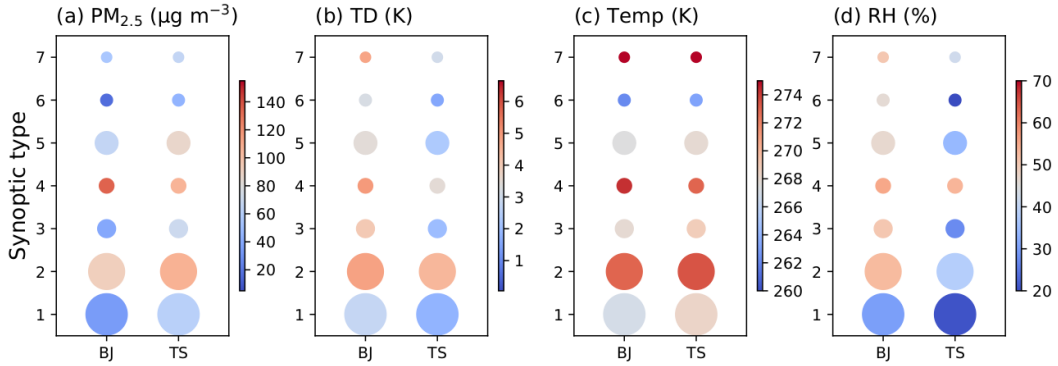

Fig. 4. (a) Average $PM_{2.5}$ concentrations under different synoptic conditions in Beijing and Tangshan, and associated (b) thermal differences (TD) of PT between 100 m and 1000 m, and (c) temperature at 1000 m, and (d) relative humidity (RH) at 200 m. The TD equals PT at 1000 m minus PT at 100 m. The size of circle represents the occurrence frequency of each synoptic type. All the meteorological variables shown are derived from the radiosonde data.

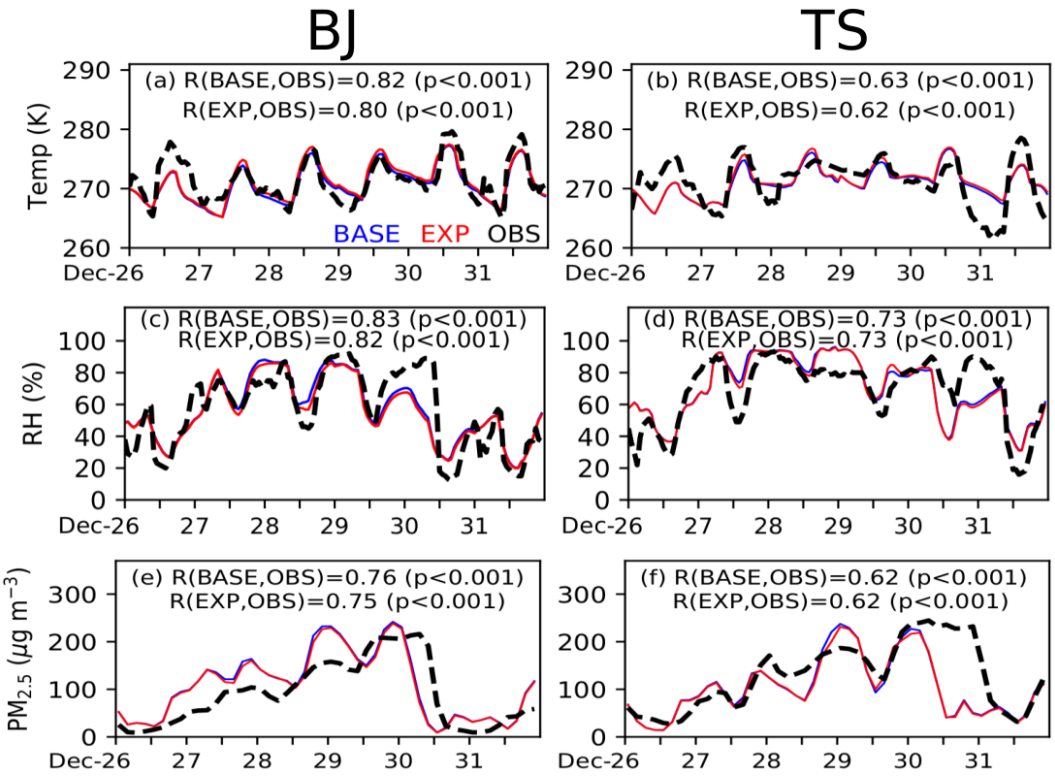

Fig. 6. Time series of observed and simulated (a, b) 2 m temperature, (c, d) 2 m RH, and (e, f) $PM_{2.5}$ concentration in (left) Beijing and (right) Tangshan from 26 to 31 December 2017. The simulations of BASE run are denoted in blue lines, and those of EXP run are denoted in red lines. The correlation coefficients (R) between the observations and simulations are also given for each panel.

3. Many previous studies on aerosols' impact on PBL have highlighted the important role of absorbing aerosol (Huang et al., 2018), did it also hold true in these two typical pollution events discussed here? Furthermore, the vertical profile of aerosol, which is highly dependent on synoptic condition, has been proven to play a vital role in aerosols' impacts on PBL development (Wang et al., 2018). It is a very crucial feature related to both synoptic weather and also PBL evolution. Thus, this work could be greatly improved by drilling down further into the link among synoptic condition, aerosol vertical structure and its impact on PBL, and in turn air pollution itself.

Yes, the absorbing aerosol played an important role in the PBL structure and aerosol pollution during the selected episode, due to the considerable amount of light-absorbing components in the aerosols of northern China (Ding et al., 2016). In the revised

manuscript, the critical roles of absorbing aerosols were discussed and the recommended literatures were properly cited.

Besides, the links among synoptic condition, aerosol vertical structure and PBL at the end of December 2017 were analyzed. The BTH was influenced by the synoptic Type 4 on December 27, which turned into the synoptic Type 2 on December 28-29 (Figs. 7 and 9). Both Types can lead to the warming of upper air and the suppression of PBL (Figs. 7), favoring the accumulation of pollutants (Figs. 7, 9a-b and 10c-d). These results indicated that the evolution of synoptic pattern provided the primary driving force for the day-to-day variations of aerosol concentrations during the studied episode. Also, influencing by the Types 4 and 2, prominent perturbations induced by the aerosol radiative effect on the BLH and $PM_{2.5}$ concentrations could be found (Fig. 9c-f). It seems that Type 2 is more conducive for the aerosol radiative feedback (Figs. 10 and 11) than Type 4. Comparing with Type 2, the Type 4 induced a stronger thermal stability in the lower troposphere (Figs. 10a-b and 11a), and trapped more aerosols below 400 m AGL (Figs. 10c-d and 11b). By contrast, more aerosols were transported to upper levels under Type 2 (Figs. 10c-d and 11b), which can enhance the aerosol-PBL radiative feedback (Figs. 10e-f and 11c) due to the stronger solar radiation and weaker turbulence at the upper levels close to the PBL top (Wang et al., 2018).

In the revised manuscript, the relevant analyses and discussions were added in the Section 3.2.

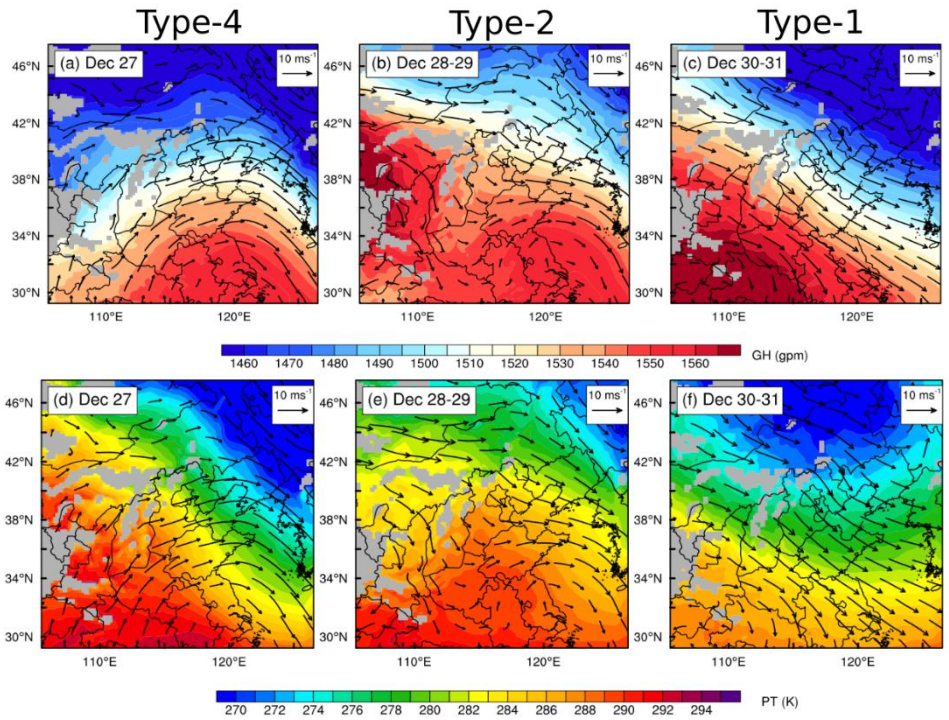

Fig. 7. Simulated 850-hPa (a-c) GH and (d-f) PT fields on December 27, 28-29 and 30-31, overlaid with the wind vectors. The regions with terrains higher than the 850-hPa level are marked by the grey shadings.

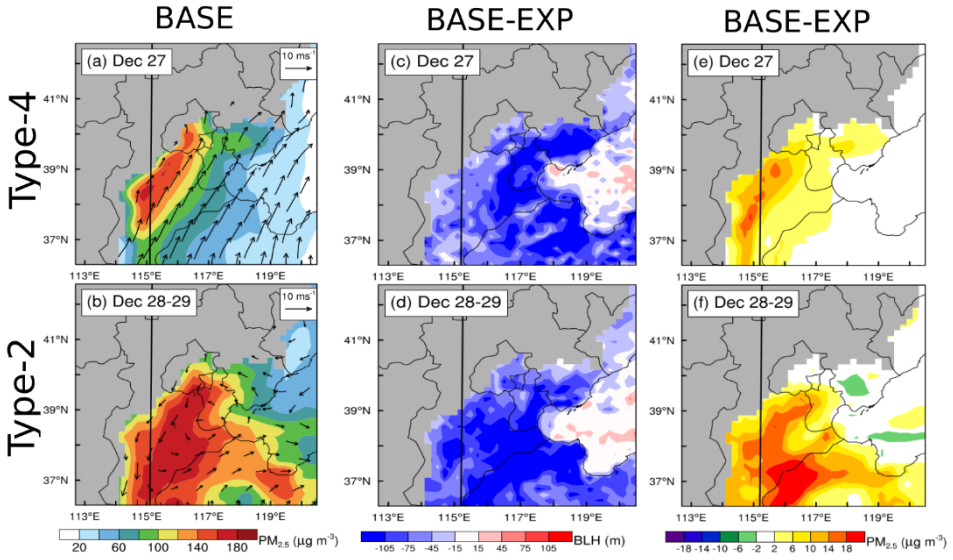

Fig. 9. Spatial distribution of simulated (a, b) near-surface $PM_{2.5}$ concentration and wind, and the perturbations induced by the aerosol radiative effect on (c, d) BLH and (e, f) $PM_{2.5}$ in the plains of BTH during 0900 to 1600 BJT on (top) December 27 and (bottom) December 28-29. The black lines in Fig. 9a indicates the locations of vertical sections shown in Fig. 10.

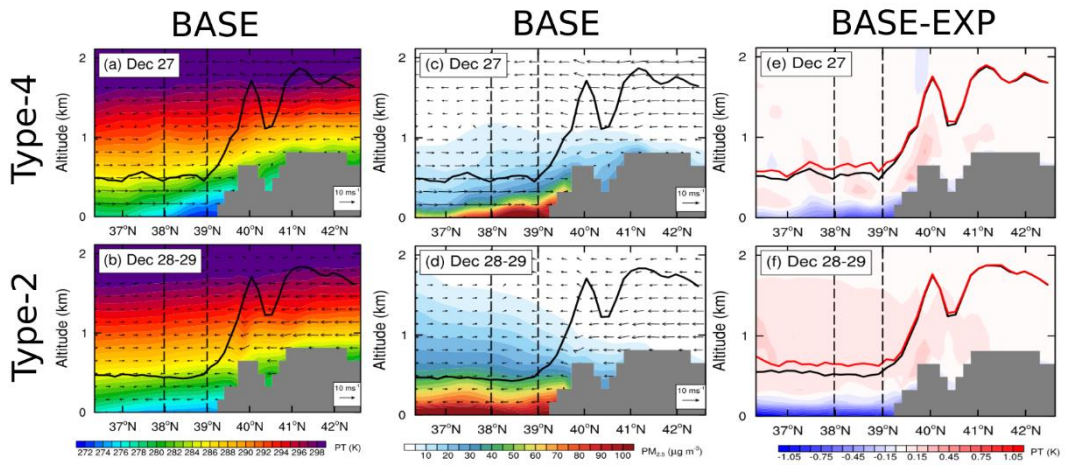

Fig. 10. Vertical cross sections of simulated (a, b) PT, (c, d) $PM_{2.5}$ concentration, and (e, f) the concentration perturbation induced by the aerosol radiative effect during 0900 to 1600 BJT on (top) December 27, and (bottom) December 28-29. The locations of cross section are indicated by the black lines in Fig. 9. In Fig. 10e-f, the BLH of BASE run is denoted by the black lines, and the BLH of EXP run is denoted by the red lines. Note that the vertical velocity is multiplied by a factor of 10 when plotting the wind vectors. The vertical dashed lines indicate the regions to derive the profiles of PT and $PM_{2.5}$ concentration shown in Fig. 11.

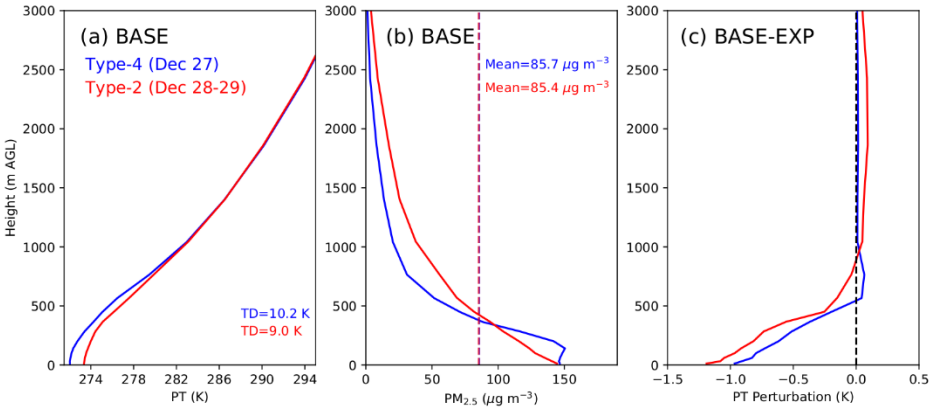

Fig. 11. Average vertical profiles of simulated (a) PT, (b) $PM_{2.5}$ concentration, and (c) PT perturbations induced by the aerosol radiative effect during 0900 to 1600 BJT on December 27 (in blue) and December 28-29 (in red), derived from the simulations along the cross section shown in Fig. 10 between 38 °N and 39 °N. In Fig. 11a, the TD is calculated as the PT difference between 100 m and 1000 m. In Fig. 11b, the dash lines indicate the mean $PM_{2.5}$ concentrations below 3000 m AGL on December 27 (in blue) and December 28-29 (in red).

Minor corrections:

Line 63: In the sentence "…leading to lower the BLH and deteriorate the pollution", "to" is a preposition and should be followed by substantive expressions instead of the root form of a verb.

Thanks, the sentence was revised as: "…the massive aerosols can intensify the PBL stability through scattering the solar radiations, which can lower the BLH and deteriorate the pollution".

Line 66: "…meteorological driving for" should be "…meteorological driving factor for ".

Thanks, the sentence was revised as suggested.

Line 77: "green triangle" should be in plural form.

Revised as suggested.

Line 85: "… has been widely to …" should be "… has been widely applied to …".

Revised as suggested.

Line 88: The same problem as Line 63, "in consideration of" should be followed by substantive expressions not an independent sentence.

The sentence was revised as: "Considering that the heavy $PM_{2.5}$ pollution events primarily occurred during winter …"

Line 116: According to Fig. 2, it seems that not all the warming of upper air leads to a pollution aggravation (such as the time period at the end of November). Are there any other factors to be mentioned that control the variations of particulate matter in BTH? Besides, the author only gives the variations of potential temperature, while the definition of inversion is more concerned about air temperature. The vertical structure of air temperature may also worth attention.

To understand the relationships between the warming of upper air and the variations of

$PM_{2.5}$ concentration, we compared the daily variations of $PM_{2.5}$ concentration ($\Delta PM_{2.5}$) and those of 1300-m PT (ΔPT) in Beijing in November and December 2017. As shown in Fig. R2, there were 32 days associated with the warming of upper air over Beijing, and all these days were corresponding to the increases of $PM_{2.5}$ concentration. Similar relationship also can be found in Tangshan, which implies the critical role of thermal stability in the aerosol pollution of BTH during winter.

Thanks for your kind suggestion, in the revised manuscript the vertical structure of air temperature (Fig. 4) were also examined to further understand the relationships between PBL thermal structure and aerosol pollution.

We agreed with the reviewer that in addition to the local PBL thermal structure, there are other factors that influence the aerosol pollution level in BTH, such as the transport of pollutants. Thus, in the revised manuscript, the transport of pollutants associated with the synoptic Type 4 during the selected episode were analyzed and discussed in the Sections 3.1 and 3.2.

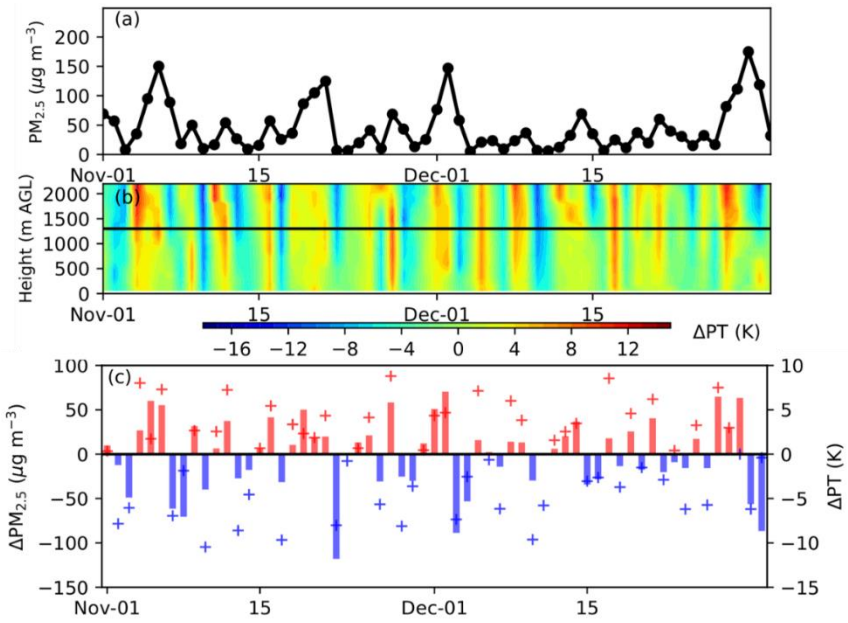

Fig. R2 (a) Time series of observed $PM_{2.5}$ concentration from 1 November to 31 December in 2017 in Beijing, and (b) the 24-hr variations of potential temperature (ΔPT) derived from the sounding data at 2000 BJT. In Fig. R2c, the daily variations of $PM_{2.5}$ concentration ($\Delta PM_{2.5}$) are denoted by the color bars (positive values in red, negative values in blue), and those of 24-hr ΔPT at 1300 m are shown by the color pluses (positive values in red, negative values in blue).

Line 128: The total occurrence of type 1 and type 2 synoptic pattern is about 70% (Line 123), it's a little confusing why the rate of other synoptic types is no more than 12.5%. Shouldn't they be summed up to 100%?

Yes, all the types were summed up to 100%. Sorry for this ambiguous sentence, which was revised as: "Except for these two dominant types, the occurrence rate of other five synoptic types is 30.4% in total."

Line 133: The author may intend to mention "Fig. 4b" instead of "Fig. 3b" since Fig 4 gives the difference of potential temperature.

Sorry for this typo. It was corrected in the revised manuscript.

Line 155: "resulting to" should be corrected to "resulting in".

Revised as suggested.

Figure 1 caption: "green triangle" should be in plurality, i.e. "green triangles".

Revised as suggested.

Section 3.3 is too short to be a subsection

The Section 3.3 was merged into the previous section as suggested.

Reference:

Chan C et al., Air pollution in mega cities in China, Atmos. Environ., 2008, 42, 1–42, doi:10.1016/j.atmosenv.2007.09.003, 2008.

Ding et al., Enhanced haze pollution by black carbon in megacities in China, Geophys. Res. Lett., 2016, 43, doi:10.1002/2016GL067745

Hu X et al., Impact of the Loess Plateau on the atmospheric boundary layer structure and air quality in the North China Plain? A case study, Sci. Total Environ., 2014, 499, 228–237, doi:10.1016/j.scitotenv.2014.08.053

Huang X et al., Impact of Aerosol-PBL Interaction on Haze Pollution: Multiyear

Observational Evidences in North China. Geophysical Research Letters, 2018, 45(16): 8596-8603.

Miao Y et al., Classification of summertime synoptic patterns in Beijing and their associations with boundary layer structure affecting aerosol pollution, Atmos. Chem. Phys., 2017, 17(4), 3097–3110

Wang Z et al., Dome effect of black carbon and its key influencing factors: a one-dimensional modelling study. Atmospheric Chemistry and Physics, 2018, 18(4): 2821-2834.

Wei P et al., Impact of boundary-layer anticyclonic weather system on regional air quality, Atmos. Environ., 2011, 45, 2453–2463, doi:10.1016/j.atmosenv.2011.01.045.

Ye X et al., Study on the synoptic flow patterns and boundary layer process of the severe haze events over the North China Plain in January 2013, Atmos. Environ., 2016, 124, 129–145.

Zhang J et al., The impact of circulation patterns on regional transport pathways and air quality over Beijing and its surroundings, Atmos. Chem. Phys., 2012, 12, 5031–5053, doi:10.5194/acp-12-5031-2012.

Zhang Y et al., Impact of synoptic weather patterns and inter-decadal climate variability on air quality in the North China Plain during 1980–2013. Atmospheric environment, 2016, 124: 119-128.

Integrated impacts of synoptic forcing and aerosol radiative effect on boundary layer and pollution in the Beijing-Tianjin-Hebei region, China

Yucong Miao[1], Huizheng Che[1], Xiaoye Zhang[1], Shuhua Liu[2]

[1]State Key Laboratory of Severe Weather & Key Laboratory of Atmospheric Chemistry of CMA, Chinese Academy of Meteorological Sciences, Beijing 100081, China
[2]Department of Atmospheric and Oceanic Sciences, School of Physics, Peking University, Beijing 100871, China

Correspondence to: H. Che (chehz@cma.gov.cn) and X. Zhang (xiaoye@cma.gov.cn)

Abstract. Rapid urbanization and industrialization have led to deterioration of air quality in the Beijing-Tianjin-Hebei (BTH) region with high loadings of $PM_{2.5}$. The heavy aerosol pollutions frequently occur in winter, closely in relation to the planetary boundary layer~~-~~ (PBL) meteorology~~meteorological conditions~~. To unravel the physical~~complicated impacts of large scale processes that influences the atmospheric forcing and the local scale planetary boundary layer (~~PBL structure and aerosol pollution~~)~~ ~~characteristics on the pollution~~ in BTH~~there~~, this study combined long-term observational data analyses, synoptic pattern classification, and meteorology-chemistry coupled simulations. During the winter of 2017 and 2018, Beijing~~, Langfang, Tianjin,~~ and Tangshan often ~~simultaneously~~ experienced heavy $PM_{2.5}$ pollution simultaneously, accompanying with strong thermal inversion aloft. These concurrences of pollution in different cities were primarily regulated by the large-scale ~~atmospheric processes~~synoptic condition. Using the principal component analysis with the geopotential height fields at the 850-hPa level during winter, two~~the~~ typical ~~polluted~~ synoptic patterns associated with heavy pollution in BTH were~~as~~ identified. One~~The~~ pattern is characterized~~was featured~~ by a southeast-to-north pressure gradient across the BTH, and the other is associated with the high-pressure in eastern China. Both synoptic types are featured by warmer air temperature at 1000 m AGL, which could suppress the development of PBL~~westerly winds from upstream mountainous regions. By inducing warm advections from the west, the thermal inversion aloft in the BTH could be enhanced, leading to shallow daytime PBLs and high near-surface $PM_{2.5}$ concentrations~~. Under these unfavourable synoptic conditions~~In addition~~, the aerosols can~~may also~~ modulate the PBL structure through the~~its~~ radiative effect, which was examined using numerical simulations. The aerosol radiative effect can significantly lower the daytime boundary layer height~~ in the afternoon~~ through cooling the surface layer and heating the upper part of PBL, leading to the deterioration of air quality. And this PBL-aerosol feedback is sensitive to the aerosol vertical structure, which would be more effective when the synoptic pattern can distribute more aerosols to the upper PBL.~~Thus, more aerosols could be accumulated in the lower portion of PBL, bringing about heavy pollution in the BTH. This study has revealed the important roles played by the meteorology-aerosol interaction on the air quality.~~

1 Introduction

The Beijing-Tianjin-Hebei (BTH) region is the national capital region of China, and covers an area of ~217,156 km^2 in the North China Plain. During the last few decades, the BTH has experienced prosperous economic growth and intensive urban expansion, and becomes one of most developed and populous regions in China. Along with the tremendous development, pollution events with massive $PM_{2.5}$ (airborne particles with aerodynamic diameter less than 2.5 μm) frequently occur in the BTH, due primarily to the high emissions (Cheng et al., 2016; Geng et al., 2017; Zhang et al., 2013).

The fate of emitted pollutants is largely governed by the planetary boundary layer (PBL) (Garratt, 1994; Miao and Liu, 2019; Oke, 2002; Stull, 1988), which is the region of the lower troposphere and strongly influenced by the surface. The PBL acts as changeable coupling agents that modulate momentum, heat, moister, and matter between the surface and free troposphere (Baklanov et al., 2011; Miao et al., 2019a; Stull, 1988). In the vertical dimension, the intensity of thermal buoyancy is controlled by the thermal stratification, and the strength of mechanical turbulence is determined by the surface roughness and the PBL wind. Together these thermal and mechanical PBL processes determine the vertical dispersion and dilution of pollutants and the air replacing from upper levels (Miao et al., 2019a; Oke, 2002; Stull, 1988). Thereby, the depth of PBL, also known as the boundary layer height (BLH), has been extensively utilized to characterize the atmospheric environmental capacity and the dilution volume of pollutants (Stull, 1988; Seidel et al., 2010; Hu et al., 2014; Miao et al., 2015).

Through observational experiments and numerical simulations, the ~~associations~~ connections between the PBL characteristics and aerosol pollution in the BTH have been investigated (e.g., Miao et al., 2019b; Quan et al., 2013; Wang et al., 2018a; Ye et al., 2016; Zhong et al., 2017, 2018). The heavy $PM_{2.5}$ pollution events in BTH typically occur under stagnant situations with shallow PBL (Ye et al., 2016; Zhong et al., 2017 and 2018). On a seasonal basis, the heaviest aerosol pollution in BTH occurs in winter, which is not only ascribed to the seasonal changes in emissions and precipitation, but also the shifts in the BLH (Miao et al., 2015, 2018b). With mountains and seas surrounded (Fig. 1), the PBL process/structure and pollution level in the BTH are usually impacted by the geographical forcings (Chen et al., 2009; Hu et al., 2014, 2016, Miao et al., 2015, 2016, 2017b). Due to the blocking effects of mountains, the momentum exchanging processes between the PBL and the upper free troposphere could be repressed dynamically (Miao et al., 2018; Wang et al., 2018b). Moreover, the local thermal gradient between the mountains-and-plains or land-and-sea can bring on closed circulation systems, and modify the near-surface winds and thermal inversion intensity, leading to the re-circulation and accumulation of pollutants (Chen et al., 2009; Miao et al., 2015, 2017b, 2019a).

In addition to these local-scale surface factors/processes (e.g., friction, thermally induced wind systems, heat fluxes), the large-scale synoptic pattern (e.g., transient systems, thermal advections) plays a role in supplying the foremost driving for the day-to-day variations of BLH and pollution (Hu et al., 2014; Miao et al., 2019b; Stull, 1988; Zhang et al., 2016). Based on the 850-hPa geopotential height (GH) data from 1980 to 2013, Zhang et al. (2016) elucidated the potential linkages between East Asian Monsoon, synoptic condition, and air pollution in the North China Plain. They found that the stagnant weather condition with southerly and westerly winds would worsen the air quality in North China Plain, and the occurrence of stagnant condition was

relevant to the inter-annual and inter-decadal variability of monsoon. The regional transport of pollutants induced by the large-scale synoptic condition is critical to the air quality (Zhang et al., 2019). Although the previous studies have recognized the importance of synoptic pattern and PBL meteorology ~~characteristics~~ for the aerosol pollution in the BTH, most of them focused on the short-term episodes or a specific city ~~processes in a specific city~~ (e.g., Miao et al., 2019b; Quan et al., 2013; Tie et al., 2015; Wang et al., 2019; Zhong et al., 2017). More investigations are warranted concerning (1) the typical synoptic patterns and (2) their impacts on the ~~unfavorable~~ PBL characteristics and vertical distribution of aerosols ~~of heavy pollution concurring in several cities of~~ BTH~~, and (2) the relevant synoptic conditions~~. These aspects are yet to be clearly known, partly due to the absence of continuous PBL observations ~~in the different major cities in the BTH~~. In this study, the link among synoptic condition, PBL structure, and ~~-~~aerosol pollution ~~associations~~ in the BTH will be examined using the long-term radiosonde measurements collected in Beijing and Tangshan (Fig. 1b): one close to the mountains and the other adjacent to the Bohai Sea. On the other hand, during the heavy pollution events, the light-absorbing aerosols ~~black carbon~~ can cause the upper layer of PBL to be relatively warm (Ding et al., 2016), and the massive aerosols can intensify the PBL stability through scattering the solar radiations, which can lower the BLH and ~~leading to lower the BLH and~~ deteriorate the pollution (Miao et al., 2019a; Quan et al., 2013; Sun et al., 2019; Wang et al., 2019; Zhong et al., 2017, 2018). For instance, the unfavorable PBL meteorology and the feedback of aerosol together, were found to be responsible for ~84% of the explosive growth of $PM_{2.5}$ concentration in Beijing during December 2016 (Zhong et al., 2017). The radiative effect of black carbon on PBL is quite sensitive to the vertical distribution of aerosols, which is also modulated by the synoptic pattern (Wang et al., 2018c).

Considering that the large-scale synoptic forcing is the first-order meteorological driving factor for the pollution formation/dissipation, it would be necessary to examine the impacts of aerosol radiative effect on BLH on the basis of synoptic ~~pattern~~ analyses. Thus, this study will objectively classify the synoptic patterns over the BTH during winter from 2017 to 2018, and then evaluate the integrated impacts of aerosol radiative effect on PBL structure under typical synoptic conditions using the meteorology-chemistry coupled simulations. The combination of large-scale synoptic analyses and numerical simulations allows us to understand the complicated meteorology-aerosol interaction in the BTH within an integrated framework.

2 Data and Methods

2.1 Data and synoptic classification

The aerosol pollution levels in BTH are indicated by the hourly measurements of $PM_{2.5}$ mass concentration from 2017 to 2018 in ~~four major cities, including~~ Beijing~~, Langfang, Tianjin,~~ and Tangshan (Fig. 1b). For each studied city, there are three $PM_{2.5}$ monitoring sites (illustrated by red crosses in Fig. 1b) carried out by the China National Environmental Monitoring Center (CNEMC). Besides, the radiosonde measurements in Beijing and Tangshan were collected to elucidate the complex associations between the PBL meteorology and aerosol pollution. The sounding stations (illustrated by green triangles in Fig. 1b) are equipped with the L-band radiosonde system (Miao and Liu, 2019), which can provide the vertical profiles of pressure, moisture, air temperature, and wind with a fine resolution (~10 m). The sounding balloons are conventionally launched at 0800

and 2000 Beijing Time (BJT) during a day. In addition, the surface meteorological observations (illustrated by black dots in Fig. 1b) were also obtained ~~in all the studied cities~~.

To unravel the predominant synoptic conditions related to the heavy aerosol pollution in the BTH, the 850-hPa geopotential height (GH) fields were analyzed, which were extracted from the National Centers for Environmental Prediction (NCEP) global Final (FNL) reanalysis. The studied region was centred the BTH, covering an area of 106-126 °E in longitude and 29-49 °N in latitude (Fig. 1a), and this is also the region used in the meteorology-chemical coupled simulations. Using the T-mode principal component analysis (T-PCA) (Huth, 1996; Miao et al., 2017a; Philipp et al., 2014), the dominant synoptic patterns in the BTH were objectively classified. The T-PCA has been widely applied to ~~analyze~~analyse the regional air pollutions from the synoptic perspective, and demonstrated to be a dependable approach to ravel out the influences of large-scale atmospheric forcing (e.g., Miao et al., 2017a; Stefan et al., 2010; Zhang et al., 2012). ~~In~~ Ceonsider~~ing that~~ation of the heavy $PM_{2.5}$ pollution events primarily occurred during winter (Miao et al., 2018), the daily GH fields in the winter months (January, February, November, December) of 2017 and 2018 were classified in this study. In total, 240 daily GH fields were classified.

2.2 Meteorology-chemistry coupled simulations

After identifying the typical polluted synoptic pattern, ~~two~~ a typical pollution episode~~s (EP1 and EP2 in Fig. 2)~~ that occurred from 26 to 31 ~~in~~ December 2017 wa~~s~~~~ere~~ selected and simulated using the Weather Research and Forecasting model coupled with Chemistry (WRF-Chem) (Grell et al., 2005). ~~The WRF-Chem simulations were designed to understand how the large-scale synoptic forcings impact the PBL characteristics and to what extent the aerosol radiative effect influences the BLH and pollution level.~~

T~~In t~~he model~~WRF-Chem simulations, two one-way nested~~ domain centred the BTH and covered the most mainland China ~~s~~ with a horizontal resolution~~s~~ of 17.5~~33~~ km ~~and 6.6 km were used~~ (Fig. 1a)~~, and the inner domain covered the whole BTH (Fig. 1b)~~. The model top was set to the 10-hPa level, and 33 vertical layers were configured below the top. To resolve the PBL structure, ~~-~~15 vertical layers were set below 2 km above ground level (AGL). For the simulation of chemistry processes, the RADM2-MADE/SORGAM chemical mechanism (Ackermann et al.,1998; Schell et al., 2001; Stockwell et al., 1990) ~~CBMZ mechanism and MOSAIC aerosol scheme (Zaveri, 1999; Zaveri et al., 2008)~~ were used with the Multi-resolution Emission Inventory for China (MEIC) of 2016, which is the most updated and extensively utilized anthropogenic emission data. The physics parameterization schemes used in this work included the Noah~~OAH~~ land surface scheme (Chen and Dudhia, 2001), the Mellor-Yamada PBL scheme (Nakanishi and Niino, 2006), the WRF Single-Moment-5-class (WSM5) scheme (Hong et al., 2004), the Betts-Miller-Janjic cumulus scheme (Janjić, 1994), and the updated rapid radiation scheme considering the aerosol radiative effect (Iacono et al., 2008). The initial and boundary conditions (IBCs) of meteorological parameters were configured using the NCEP-FNL reanalysis, and the IBCs of chemical variables were derived from the global model output (http://www.acom.ucar.edu/wrf-chem/mozart.shtml).

The simulations used abovementioned configurations are referred to as the BASE runs, and numerical experiments that turned off the aerosol radiative option were conducted to evaluate the impacts of aerosol radiative effect. These sensitivity experiments are regarded as the EXP runs hereunder. According to the common strategy for the Air Quality Model Evaluation International Initiative (AQMEII), the selected pollution episodes were simulated as a sequence of four-day time slices (Forkel et al., 2015), including Slice-1 (2000 BJT 24 December to 2300 BJT 28 December) and Slice-2 (2000 BJT 27 December to 2300 BJT 31 December). The first 24-h simulations of each time slice were considered as the spin-up period, and the chemical initial state of each time slice is adopted from the final state of the previous time slice if available.

3 Results and Discussion

3.1 Linkages between synoptic condition, thermal stability and $PM_{2.5}$ pollution

The time series of daily $PM_{2.5}$ concentrations in Beijing and Tangshan from 1 November to 31 December in 2017 are shown in Figs. 2a ~~and 2c~~, demonstrating several heavy pollution episodes ~~in the~~ in the BTH. It is worth noting that ~~all the studied cities~~Beijing and Tangshan often experienced heavy pollution simultaneously. Comparing with the observed potential temperature (PT) profiles in Beijing and Tangshan (Figs. 2b ~~and 2c~~d), it is clear that the quick increase (decrease) of $PM_{2.5}$ concentrations usually accompanied with the warming (cooling) of atmosphere above 1000 m AGL. The warming of upper air also could be observed from the vertical profiles of temperature, and was often accompanied with high relative humidity within the PBL (Fig. S1). The concurrence of warming aloft and increased $PM_{2.5}$ concentration~~Such a phenomenon~~ not only occurred from November to December in 2017, but also in other winter months during 2017 and 2018 (Figs. S21-S43). Given that the ~~long~~ distance between Beijing and Tangshan is as long as ~~(~~~200 km~~)~~, the synchronous change of aerosol concentrations ~~in all the four cities,~~ and the concurrence of strong thermal inversion aloft, must be relevant to certain large-scale synoptic patterns (Miao et al., 2018). Therefore, it would be necessary to investigate the $PM_{2.5}$ pollution and its influencing factors from the point of view of ~~the large-scale conditions~~synoptic condition.

Based on the 850-hPa daily GH fields in winter from 2017 to 2018, the synoptic conditions were classified using the T-PCA (Fig. 3). There are two dominant synoptic patterns ~~, the~~ type 1 and type 2, which account~~s~~ for ~70% of the total. The synoptic type 1 occurs most frequently (39.6%). There is a strong southwest-to-northeast pressure gradient across the BTH, supporting ~~to~~ strong northwesterly prevailing winds at the 850-hPa level (Fig. 3a). The average daily $PM_{2.5}$ concentrations in Beijing and Tangshan under type 1 are 34 and 62 μg m^{-3}, respectively (Fig. 4a). ~~For~~ Under the synoptic type 2, with a southeast-to-north ~~high~~ pressure gradient across the BTH at the 850-hPa level~~system to the southeast of BTH and low pressure system to the north~~, it is the westerly winds dominated over the BTH (Fig. 3b). The occurrence frequency of type 2 is 30%, ranking second among all the identified synoptic types.~~,~~ The average daily $PM_{2.5}$ concentrations in Beijing and Tangshan under the type 2 are significantly higher than those under type 1 (Fig. 4a), which are 92 and 108 μg m^{-3}, respectively. Except for these two dominant types, the occurrence rate of other five synoptic types is ~~no more than~~ 3012.45% in total. Among these five less occurred types, it's worth noting that the synoptic type 4 has the highest average $PM_{2.5}$ concentrations (135 μg m^{-3} in Beijing and 106 μg m^{-3}

in Tangshan), despite its occurrence frequency is merely 5.0 % (Figs. 3d and 4a). Under synoptic type 4, influencing by a high-pressure in eastern China at the 850-hPa level (Fig. 3d), the southerly prevailing winds can cause regional transport of pollutants to Beijing and Tangshan (Miao et al., 2017a; Zhang et al., 2019). To understand the connection between synoptic pattern and PBL structure, the

~~Fig. 4a exhibits the averaged $PM_{2.5}$ concentrations of each identified synoptic type in all the studied cities. Distinct difference could be found between the type 1 and type 2. The averaged $PM_{2.5}$ concentrations of type 1 are less than 62 μg m^{-3}, while type 2 is associated with heavier pollution with averaged concentrations greater than 92 μg m^{-3}. Based on the observed PT profiles, the~~ thermal stabilities~~y~~ between 100 m and 1000 m AGL ~~of each pattern were~~ are compared~~estimated as the difference between the PT values at 100 m and 1000 m AGL~~ (Fig. 4~~3~~b). ~~Comparing with the synoptic type 1, S~~stronger ~~thermal~~ stabilities are observed under ~~the~~ type 2 and type 4~~in both Beijing and Tangshan~~, associated with warmer air temperature at 1000 m AGL (Fig. 4b-c), suppressing the development of PBL (Miao et al., 2017a; Hu et al., 2014). Also, moister air could be observed within the PBL under these two types (Fig. 4d), favouring the formation of secondary inorganic aerosols (Zhong et al., 2017 and 2018). ~~.~~Thus, among all the identified patterns, the synoptic type 2 and type 4 are~~can be~~ regarded as the representative polluted pattern ~~in the BTH, due to its high occurrence frequency, high $PM_{2.5}$ concentration, and strong thermal stability~~. In the next section, a pollution episode associated with type 2 and type 4 will be investigated.~~.~~

3.2 ~~Typical polluted~~ Integrated impacts of synoptic pattern and aerosol radiative effect during the selected episode~~PBL structure~~

To unravel the complicated processes leading to the heavy pollution under ~~the~~ synoptic type 2 and type 4, a~~two~~ pollution episode~~s~~ occurred at the end of ~~in~~ 2017 was~~ere~~ selected and simulated using the WRF-Chem model~~, which were the EP1 (November 30 to December 5) and the EP2 (December 26 to 31)~~. Fig. 5 presents the vertical structure of simulated PT in Beijing and Tangshan during the~~those selected~~ episode~~s~~. Comparing with the observed PT profiles ~~shown in Figs. 2b and 2d~~, the warmings of atmosphere aloft from 27 to 29 December ~~during December 1-2 and December 28-29~~ in both Beijing and Tangshan were well simulated, with~~.~~ correlation coefficients of 0.91 ($p<0.001$) in Beijing and 0.94 ($p<0.001$) in Tangshan~~Furthermore~~,~~,~~ T~~t~~he changes of wind profile in Beijing and Tangshan ~~during those episodes~~ were also accurately reproduced ~~simulated (Fig. S4)~~, with correlation coefficients greater than 0.64~~73~~ for both the zonal and meridional winds. In Fig. 6, the simulated near-surface temperature, relative humidity, and $PM_{2.5}$ concentration are validated against the observations ~~in all the four studied cities~~. Although discrepancies exist, the simulated temperature, humidity, and $PM_{2.5}$ all demonstrate rationally good agreement with the observations. Besides, comparing the simulations with aerosol radiative effect to those without, the former presents higher $PM_{2.5}$ concentrations, lower temperatures, and higher humidities, resulting in higher correlation coefficients with observations (Fig. 6). Overall, t~~T~~h~~e~~ese good model performances ~~of WRF-Chem~~ (Figs. 5-6 ~~and S4~~) provide a solid basis to utilize the ~~model data~~simulation results to elucidate the physical mechanisms underlying the ~~heavy~~ pollution episode.

Based on the model output, the BLH is estimated as the height where the PT first surpasses the minimum PT below by 1.5 K (Nielsen-Gammon et al., 2008; Seidel et al., 2010). The same BLH derivation method has been widely employed in previous PBL studies (e.g., Hu et al., 2014; Miao and Liu, 2019; Nielsen-Gammon et al., 2008), which can explicitly manifest the influences of thermal stability. ~~As the estimated BLH shown in~~ Fig. 5 shows the time series of simulated BLH in Beijing and Tangshan.~~,~~ ~~I~~it is clear that the ~~strengthening of thermal inversion~~warmings of upper air can suppresses the daytime BLH~~, and favors the accumulation of pollutants. During the EP1, the warming processes of atmosphere above PBL on December 1-2 was associated with the synoptic type~~ on December 27 under synoptic type 4 and on December 28-29 under synoptic type 2~~2~~ (Fig. 7a-b). On December 27, i~~I~~nfluencing by the southwesterly winds, the warmer air mass ~~over the western mountainous regions~~ could be brought to the BTH (Figs. 7d~~c and 8a~~). ~~Such a warm advection~~ enhanc~~inged~~ the thermal stability and restrain~~inged~~ the growth of PBL ~~in the BTH~~ (Figs. 8a). The southwesterly prevailing winds ~~and 9a),~~ can transport the pollutants emitted from upstream plain regions to the BTH and further worsen the air quality ~~resulting to high $PM_{2.5}$ concentrations at the ground level~~ (Figs. 8d~~c~~ and 9a~~e~~). Then, ~~the~~ the synoptic condition transitioned to type 2 on December 28-29, and the strong thermal inversion and shallow PBL situation in BTH could last until the outbreak of cold advection on December 30 (Figs. 6, 7 and 8). As shown in Fig. 8a-c, the average BLH in BTH was suppressed to less than 250 m under synoptic type 4 and type 2 from 27 to 29 December, and then increased to 500 m from 30 to 31 December. As a result, massive aerosols were accumulated in the plains of BTH from 27 to 29 December (Figs. 8e and 9b).~~For example, on December 2 the daytime BLH was suppressed to less than 500 m in both Beijing and Tangshan (Fig. 5). By contrast, the daytime PBL could reach a height greater than 1500 m on December 3-4 under the synoptic type 1 (Figs. 5 and 7b). On December 3-4, the induced northwesterly cold advection not only facilitated the horizontal dispersion of pollutants, but also weakened the thermal inversion and favored the development of PBL in the BTH (Figs. 7d, 8b, and 9b), leading to relatively good air quality there (Figs. 8d and 9d). Similar evolutions of synoptic situation and PBL structures could also be noted during the EP2. On December 28-29, the synoptic type 2 induced strong thermal inversions, shallow PBLs and high $PM_{2.5}$ concentrations in the BTH, while on December 30-31 the appearance of type 1 led to the dissipation of the pollutants (Figs. 10, S5 and S6).~~

~~3.3 Impact of aerosol radiative effect on the PBL structure and pollution~~

~~In addition to the large-scale warm/cold advections~~During those heavy polluted days, the suspended aerosols ~~-~~may also modify the PBL structure in BTH to some extent (Gao et al., 2015; Wang et al., 2018c; Miao et al., 2019a; Zhong et al., 2018). As the aerosols reduce the solar radiation reaching the ground, the development of PBL could be suppressed, particularly during the daytime. As shown in Fig. 9c-d~~11~~, ~~during the EP1~~ the aerosol radiative effect can impose significant negative perturbations on the daytime BLH. On average, the daytime BLH in the plains of BTH decreased by 84 m (15 %) on December 27 and 93 m (18 %) on December 28-29, and increased the ground-level $PM_{2.5}$ concentrations by 4.3 and 9.0 μg m^{-3}, respectively (Fig. 9e-f). The feedback on $PM_{2.5}$ was more prominent in the regions with higher concentrations, where the ground-level $PM_{2.5}$ concentration could increase by 20 μg m^{-3} during the daytime (Fig. 9e-f). Comparing the induced BLH perturbations on

December 27 with those on December 28-29, the decrease of BLH was more significant on December 28-29, which may be caused by the larger amount of aerosols suspended within the PBL on December 28-29 (Fig. 9a-b).

On the other hand, the synoptic condition can also modulate the sensitivity of PBL-aerosol feedback through influencing the vertical distribution of aerosols (Wang et al., 2018c). To elucidate the link among synoptic types and aerosol vertical structures, we examined the south-to-north cross sections of PT and $PM_{2.5}$ cutting through the most polluted region in BTH (Fig. 10). Influencing by the southerly warm advections under synoptic type 4, the lower troposphere had a stronger thermal stratification on December 27 than on December 28-29 under synoptic type 2 (Figs. 10a-b and 11a), leading to more aerosols in the lower PBL on December 27 (Figs. 10c-d). By contrast, the aerosols can be distributed more evenly in the vertical direction on December 28-29 under synoptic type 2. Fig. 11b presents the average vertical profiles of $PM_{2.5}$ concentration along the cross section between 38 °N and 39 °N, in which the total amounts of $PM_{2.5}$ were almost the same on December 27 and December 28-29 but distributed distinctly. With more aerosols at the upper levels under synoptic type 2 on December 28-29, the daytime aerosol radiative feedback on the PBL thermal structure was enhanced (Figs. 10e-f and 11c). Since the solar radiation is more intense at the upper levels, the elevated aerosol layer can absorb more solar radiations and strengthen the thermal stratification more effectively (Wang et al., 2018c; Huang et al., 2018). Thus, comparing with synoptic type 4, the type 2 can be more conducive for the aerosol radiative feedback.

~~and positive perturbations on the ground-level aerosol concentration. By averaging over the simulation results in the region of interest (ROI) shown in Fig 11, the time series of BLH and induced perturbations of $PM_{2.5}$ and PT were derived. During the most polluted day (December 2) of the EP1, the aerosol radiative effect can lower the BLH up to 160 m in the afternoon (Fig. 12a) through cooling the surface layer below 300 m AGL and heating the upper atmosphere (Fig. 12c). Consequently, more aerosols can be accumulated in the lower portion of PBL, which can increase the ground level $PM_{2.5}$ concentration by 28 μg m^{-3} (15%) (Fig. 12b). Similar influences of the aerosol radiative effect on the PBL and aerosol pollution could also be observed during the EP2 (Fig. S7 and S8), which can lower the daytime BLH by 110 m and increase the $PM_{2.5}$ concentration by 18 μg m^{-3} (10%). These simulation results indicate that under unfavorable synoptic condition the aerosol radiative effect plays a crucial role in enhancing the thermal stability within the PBL and exacerbating the pollution, which cannot be neglected.~~

4 Conclusions

To elucidate~~understand~~ the link among synoptic ~~critical roles of large-scale atmospheric~~ forcing, ~~and local-scale~~ PBL structure, and~~on the~~ aerosol pollution in the BTH, this study combined long-term observational data analyses, synoptic classification, and meteorology-chemistry coupled simulations. On the basis of the wintertime $PM_{2.5}$ measurements and radiosonde data in ~~four major cities (i.e.,~~ Beijing~~, Langfang, Tianjin,~~ and Tangshan~~)~~ from 2017 to 2018, the relationships between PBL structure~~thermal inversion~~ and aerosol pollution were examined. It was found that both cities ~~all the studied cities in the BTH~~ often experienced high $PM_{2.5}$ concentrations simultaneously, which typically accompanied with strong thermal inversion aloft.

These concurrences of heavy pollution in Beijing and Tangshandifferent cities were regulated by the large-scale synoptic forcings.

Using the T-PCA with the 850-hPa daily GH fields during winter, two the typical synoptic patterns relevant to the heavy pollution in Beijing and Tangshanthe BTH wereas identified. One is characterized by a southeast-to-north pressure gradient across the BTH at the 850-hPa level, leading to westerly prevailing winds to BTH. The other is associated with the high-pressure in eastern China and southerly prevailing winds to BTH. These two types are both featured by warmer air temperature at 1000 m AGL, which can significantly suppress the development of PBL.

With high pressure system to the southeast of BTH and low pressure system to the north, the identified pattern is featured by the 850-hPa westerly winds over the BTH. And the warmer air mass from the western mountains could be brought to the BTH, leading to enhance the thermal inversion aloft and suppress the development of daytime PBL over the plains. Comparing with the clean situations, the induced large-scale warm advections can decrease the daytime BLH by several hundred meters, resulting to a high concentration of pollutants in the whole BTH.

In addition to the large-scale warm advectionsUnder these unfavourable synoptic conditions, the aerosols suspended in the atmosphere canmay also modulate the PBL structure. ATwo pollution episodes at the end of 2017 associated with these typical synoptic typepatterns wasere selected and simulated using the WRF-Chem by turning on and off the aerosol radiative option. The simulation results indicated that the aerosol radiative effect can significantly lower the daytime BLH in the afternoon through cooling the surface layer and heating the upper part of PBL. Thereupon, more aerosols could be accumulated in the lower portion of PBL.. SSuch a PBL-aerosol feedback is sensitive to the aerosol vertical structure, which would be more effective when the synoptic pattern can distribute more aerosols to the upper PBL. At lastmechanism plays a critical role in the explosive growth of aerosol concentration under unfavorable synoptic conditions, which should not be overlooked. Besides, although this study highlights the important roles of multi-scale physical processes in the aerosol pollution in the BTH, the chemical mechanisms/processes also should not be deemphasized.

Data availability. The reanalysis data can be downloaded from http://rda.ucar.edu/datasets/ds083.2/. The meteorological data in the BTH are available from the China Meteorological Administration (http://data.cma.cn/), and the $PM_{2.5}$ data can be obtained from the CNEMC (http://www.cnemc.cn/). The model data are available by request (chehz@cma.gov.cn).

Author contributions. Development of the ideas and concepts behind this work was performed by all the authors. Model execution, data analysis, and paper preparation were performed by YM and HC with feedback and advice from XZ and SL.

Competing interests. The authors declare that they have no conflict of interest.

Acknowledgements. This study received financial support from National Natural Science Foundation of China (41705002, 41825011), Beijing Natural Science Foundation (8192054), and Atmospheric Pollution Control of the Prime Minister (DQGG0106). The authors would like to acknowledge the Tsinghua University for the support of emission data.

References

Ackermann, I.J., Hass, H., Memmesheimer, M., Ebel, A., Binkowski, F.S., and Shankar, U.: Modal aerosol dynamics model for Europe. Atmos. Environ., 32, 2981-2999, doi:10.1016/S1352-2310(98)00006-5, 1998.

Baklanov, A. A., Grisogono, B., Bornstein, R., Mahrt, L., Zilitinkevich, S. S., Taylor, P., Larsen, S. E., Rotach, M. W. and Fernando, H. J. S.: The nature, theory, and modeling of atmospheric planetary boundary layers, Bull. Am. Meteorol. Soc., 92(2), 123–128, doi:10.1175/2010BAMS2797.1, 2011.

Chen, F. and Dudhia, J.: Coupling an Advanced Land Surface–Hydrology Model with the Penn State–NCAR MM5 Modeling System. Part I: Model Implementation and Sensitivity, Mon. Weather Rev., 129(4), 569–585, doi:10.1175/1520-0493(2001)129<0587:CAALSH>2.0.CO;2, 2001.

Chen, Y., Zhao, C., Zhang, Q., Deng, Z., Huang, M. and Ma, X.: Aircraft study of Mountain Chimney effect of Beijing, China, J. Geophys. Res. Atmos., 114(8), 1–10, doi:10.1029/2008JD010610, 2009.

Cheng, Z., Luo, L., Wang, S., Wang, Y., Sharma, S., Shimadera, H., Wang, X., Bressi, M., de Miranda, R. M., Jiang, J., Zhou, W., Fajardo, O., Yan, N. and Hao, J.: Status and characteristics of ambient PM2.5 pollution in global megacities, Environ. Int., 89–90, 212–221, doi:10.1016/j.envint.2016.02.003, 2016.

Ding, A. J., Huang, X., Nie, W., Sun, J. N., Kerminen, V.-M., Petäjä, T., Su, H., Cheng, Y. F., Yang, X.-Q., Wang, M. H., Chi, X. G., Wang, J. P., Virkkula, A., Guo, W. D., Yuan, J., Wang, S. Y., Zhang, R. J., Wu, Y. F., Song, Y., Zhu, T., Zilitinkevich, S., Kulmala, M. and Fu, C. B.: Black carbon enhances haze pollution in megacities in China, Geophys. Res. Lett., 43, 1–7, doi:10.1002/2016GL067745, 2016.

Forkel, R., Balzarini, A., Baró, R., Bianconi, R., Curci, G., Jiménez-Guerrero, P., Hirtl, M., Honzak, L., Lorenz, C., Im, U., Pérez, J. L., Pirovano, G., San José, R., Tuccella, P., Werhahn, J. and Žabkar, R.: Analysis of the WRF-Chem contributions to AQMEII phase2 with respect to aerosol radiative feedbacks on meteorology and pollutant distributions, Atmos. Environ., 115, 630–645, doi:10.1016/j.atmosenv.2014.10.056, 2015.

Garratt, J.: Review: the atmospheric boundary layer, Earth-Science Rev., 37, 89–134, doi:10.1016/0012-8252(94)90026-4, 1994.

Gao, Y., Zhang, M., Liu, Z., Wang, L., Wang, P., Xia, X., Tao, M., and Zhu, L.: Modeling the feedback between aerosol and meteorological variables in the atmospheric boundary layer during a severe fog–haze event over the North China Plain, Atmos. Chem. Phys., 15, 4279–4295, doi:10.5194/acp-15-4279-2015, 2015.

Geng, G., Zhang, Q., Tong, D., Li, M., Zheng, Y., Wang, S., and He, K.: Chemical composition of ambient PM2. 5 over China and relationship to precursor emissions during 2005–2012, Atmos. Chem. Phys., 17, 9187–9203, https://doi.org/10.5194/acp-17-9187-2017, 2017.

Grell, G. A., Peckham, S. E., Schmitz, R., McKeen, S. A., Frost, G., Skamarock, W. C. and Eder, B.: Fully coupled "online" chemistry within the WRF model, Atmos. Environ., 39(37), 6957–6975, doi:10.1016/j.atmosenv.2005.04.027, 2005.

Hong, S.-Y., Dudhia, J. and Chen, S.-H.: A Revised Approach to Ice Microphysical Processes for the Bulk Parameterization of Clouds and Precipitation, Mon. Weather Rev., 132(1), 103–120, doi:10.1175/1520-0493(2004)132<0103:ARATIM>2.0.CO;2, 2004.

Hu, X.-M., Ma, Z., Lin, W., Zhang, H., Hu, J., Wang, Y., Xu, X., Fuentes, J. D. and Xue, M.: Impact of the Loess Plateau on the atmospheric boundary layer structure and air quality in the North China Plain: A case study, Sci. Total Environ., 499, 228–237, doi:10.1016/j.scitotenv.2014.08.053, 2014.

Hu, X. M., Li, X., Xue, M., Wu, D. and Fuentes, J. D.: The Formation of Barrier Winds East of the Loess Plateau and Their Effects on Dispersion Conditions in the North China Plains, Boundary-Layer Meteorol., 1–19, doi:10.1007/s10546-016-0159-4, 2016.

Huang, X., Wang, Z., and Ding, A.: Impact of Aerosol-PBL Interaction on Haze Pollution: Multiyear Observational Evidences in North China. Geophysical Research Letters, 45(16), 8596-8603, 2018.

Huth, R.: An intercomparision of computer-assited circulation classificaiton methods , Int. J. Climatol., 16(8), 893–922, doi:10.1002/(SICI)1097-0088(199608)16:8<893::AID-JOC51>3.0.CO;2-Q, 1996.

Iacono, M. J., Delamere, J. S., Mlawer, E. J., Shephard, M. W., Clough, S. A. and Collins, W. D.: Radiative forcing by long-lived greenhouse gases: Calculations with the AER radiative transfer models, J. Geophys. Res., 113(D13), D13103, doi:10.1029/2008JD009944, 2008.

Janjić, Z. I.: The Step-Mountain Eta Coordinate Model: Further Developments of the Convection, Viscous Sublayer, and Turbulence Closure Schemes, Mon. Weather Rev., 122(5), 927–945, doi:10.1175/1520-0493(1994)122<0927:TSMECM>2.0.CO;2, 1994.

Miao, Y. and Liu, S.: Linkages between aerosol pollution and planetary boundary layer structure in China, Sci. Total Environ., 650, 288–296, doi:10.1016/J.SCITOTENV.2018.09.032, 2019.

Miao, Y., Hu, X.-M., Liu, S., Qian, T., Xue, M., Zheng, Y. and Wang, S.: Seasonal variation of local atmospheric circulations and boundary layer structure in the Beijing-Tianjin-Hebei region and implications for air quality, J. Adv. Model. Earth Syst., 7(4), 1602–1626, doi:10.1002/2015MS000522, 2015.

Miao, Y., Liu, S., Zheng, Y. and Wang, S.: Modeling the feedback between aerosol and boundary layer processes: a case study in Beijing, China, Environ. Sci. Pollut. Res., 23(4), 3342–3357, doi:10.1007/s11356-015-5562-8, 2016.

Miao, Y., Guo, J., Liu, S., Liu, H., Li, Z., Zhang, W. and Zhai, P.: Classification of summertime synoptic patterns in Beijing and their associations with boundary layer structure affecting aerosol pollution, Atmos. Chem. Phys., 17(4), 3097–3110, doi:10.5194/acp-17-3097-2017, 2017a.

Miao, Y., Guo, J., Liu, S., Liu, H., Zhang, G., Yan, Y. and He, J.: Relay transport of aerosols to Beijing-Tianjin-Hebei region by multi-scale atmospheric circulations, Atmos. Environ., 165, 35–45, doi:10.1016/j.atmosenv.2017.06.032, 2017b.

Miao, Y., Liu, S., Guo, J., Huang, S., Yan, Y. and Lou, M.: Unraveling the relationships between boundary layer height and PM2.5 pollution in China based on four-year radiosonde measurements, Environ. Pollut., 243, 1186–1195, doi:10.1016/j.envpol.2018.09.070, 2018.

Miao, Y., Li, J., Miao, S., Che, H., Wang, Y., Zhang, X., Zhu, R. and Liu, S.: Interaction Between Planetary Boundary Layer and PM2.5 Pollution in Megacities in China: a Review, Curr. Pollut. Reports, doi:10.1007/s40726-019-00124-5, 2019a.

Miao, Y., Liu, S. and Huang, S.: Synoptic pattern and planetary boundary layer structure associated with aerosol pollution during winter in Beijing, China, Sci. Total Environ., 682, 464–474, doi:10.1016/j.scitotenv.2019.05.199, 2019b.

Nakanishi, M. and Niino, H.: An improved Mellor-Yamada Level-3 model: Its numerical stability and application to a regional prediction of advection fog, Boundary-Layer Meteorol., 119(2), 397–407, doi:10.1007/s10546-005-9030-8, 2006.

Nielsen-Gammon, J. W., Powell, C. L., Mahoney, M. J., Angevine, W. M., Senff, C., White, A., Berkowitz, C., Doran, C. and Knupp, K.: Multisensor estimation of mixing heights over a coastal city, J. Appl. Meteorol. Climatol., 47(1), 27–43, doi:10.1175/2007JAMC1503.1, 2008.

Oke, T. R.: Boundary Layer Climates, Routledge., 2002.

Philipp, A., Beck, C., Huth, R. and Jacobeit, J.: Development and comparison of circulation type classifications using the COST 733 dataset and software, Int. J. Climatol., doi:10.1002/joc.3920, 2014.

Quan, J., Gao, Y., Zhang, Q., Tie, X., Cao, J., Han, S., Meng, J., Chen, P. and Zhao, D.: Evolution of planetary boundary layer under different weather conditions, and its impact on aerosol concentrations, Particuology, 11(1), 34–40, doi:10.1016/j.partic.2012.04.005, 2013.

Seidel, D. J., Ao, C. O. and Li, K.: Estimating climatological planetary boundary layer heights from radiosonde observations: Comparison of methods and uncertainty analysis, J. Geophys. Res., 115(D16), D16113, doi:10.1029/2009JD013680, 2010.

Stefan, S., Necula, C., and Georgescu, F.: Analysis of long-range transport of particulate matters in connection with air circulation over Central and Eastern part of Europe, Phys. Chem. Earth, 35, 523–529, doi:10.1016/j.pce.2009.12.008, 2010.

Schell, B., Ackermann, I.J., Hass, H., Binkowski, F.S., and Ebel, A.: Modeling the formation of secondary organic aerosol within a comprehensive air quality model system. J. Geophys. Res. Atmos., 106, 28275-28293, doi:10.1029/2001JD000384, 2001.

Stockwell, W.R., Middleton, P., Chang, J.S., and Tang, X.: The second generation regional acid deposition model chemical mechanism for regional air quality modeling. J. Geophys. Res., 95, 16343, doi:10.1029/JD095iD10p16343, 1990.

Stull, R. B.: An Introduction to Boundary Layer Meteorology, edited by R. B. Stull, Springer Netherlands, Dordrecht., 1988.

Sun, T., Che, H., Qi, B., Wang, Y., Dong, Y., Xia, X., Wang, H., Gui, K., Zheng, Y., Zhao, H., Ma, Q., Du, R. and Zhang, X.: Characterization of vertical distribution and radiative forcing of ambient aerosol over the Yangtze River Delta during 2013–2015, Sci. Total Environ., 650, 1846–1857, doi:10.1016/j.scitotenv.2018.09.262, 2019.

Tie, X., Zhang, Q., He, H., Cao, J., Han, S., Gao, Y., Li, X. and Jia, X. C.: A budget analysis of the formation of haze in Beijing, Atmos. Environ., 100, 25–36, doi:10.1016/j.atmosenv.2014.10.038, 2015.

Wang, L., Wang, H., Liu, J., Gao, Z., Yang, Y., Zhang, X., Li, Y. and Huang, M.: Impacts of the near-surface urban boundary layer structure on PM2.5 concentrations in Beijing during winter, Sci. Total Environ., 669, 493–504, doi:10.1016/j.scitotenv.2019.03.097, 2019.

Wang, H., Peng, Y., Zhang, X., Liu, H., Zhang, M., Che, H., Cheng, Y. and Zheng, Y.: Contributions to the explosive growth of PM2.5 mass due to aerosol–radiation feedback and decrease in turbulent diffusion during a red alert heavy haze in Beijing–Tianjin–Hebei, China, Atmos. Chem. Phys., 18(23), 17717–17733, doi:10.5194/acp-18-17717-2018, 2018a.

Wang, X., Dickinson, R. E., Su, L., Zhou, C. and Wang, K.: PM 2.5 Pollution in China and How It Has Been Exacerbated by Terrain and Meteorological Conditions, Bull. Am. Meteorol. Soc., 99(1), 105–119, doi:10.1175/BAMS-D-16-0301.1, 2018b.

Wang, Z., Huang, X., and Ding, A.: Dome effect of black carbon and its key influencing factors: a one-dimensional modelling study, Atmos. Chem. Phys., 18, 2821–2834, doi:10.5194/acp-18-2821-2018, 2018c.

Ye, X., Song, Y., Cai, X. and Zhang, H.: Study on the synoptic flow patterns and boundary layer process of the severe haze events over the North China Plain in January 2013, Atmos. Environ., 124, 129–145, doi:10.1016/j.atmosenv.2015.06.011, 2016.

~~Zaveri, R. A.: A new lumped structure photochemical mechanism for large scale applications, J. Geophys. Res. Atmos., doi:10.1029/1999JD900876, 1999.~~

~~Zaveri, R. A., Easter, R. C., Fast, J. D. and Peters, L. K.: Model for Simulating Aerosol Interactions and Chemistry (MOSAIC), J. Geophys. Res. Atmos., doi:10.1029/2007JD008782, 2008.~~Zhang, C., Liu, C., Hu, Q. et al.: Satellite UV-Vis spectroscopy: implications for air quality trends and their driving forces in China during 2005–2017. Light Sci. Appl., doi:10.1038/s41377-019-0210-6, 2019.

Zhang, J. P., Zhu, T., Zhang, Q. H., Li, C. C., Shu, H. L., Ying, Y., Dai, Z. P., Wang, X., Liu, X. Y., Liang, A. M., Shen, H. X. and Yi, B. Q.: The impact of circulation patterns on regional transport pathways and air quality over Beijing and its surroundings, Atmos. Chem. Phys., 12(11), 5031–5053, doi:10.5194/acp-12-5031-2012, 2012.

Zhang, R., Jing, J., Tao, J., Hsu, S.-C., Wang, G., Cao, J., Lee, C. S. L., Zhu, L., Chen, Z., Zhao, Y., and Shen, Z.: Chemical characterization and source apportionment of PM2:5 in Beijing: seasonal perspective, Atmos. Chem. Phys., 13, 7053–7074, doi:10.5194/acp-13-7053-2013, 2013.

Zhang, Y., Ding, A., Mao, H., et al.: Impact of synoptic weather patterns and inter-decadal climate variability on air quality in the North China Plain during 1980–2013. Atmospheric Environment, 124, 119-128, 2016.

Zhong, J., Zhang, X., Wang, Y., Sun, J., Zhang, Y., Wang, J., Tan, K., Shen, X., Che, H., Zhang, L., Zhang, Z., Qi, X., Zhao, H., Ren, S. and Li, Y.: Relative contributions of boundary-layer meteorological factors to the explosive growth of PM2.5 during the red-alert heavy pollution episodes in Beijing in December 2016, J. Meteorol. Res., 31(5), 809–819, doi:10.1007/s13351-017-7088-0, 2017.

Zhong, J., Zhang, X., Dong, Y., Wang, Y., Liu, C., Wang, J., Zhang, Y. and Che, H.: Feedback effects of boundary-layer meteorological factors on cumulative explosive growth of PM 2.5 during winter heavy pollution episodes in Beijing from 2013 to 2016, Atmos. Chem. Phys., doi:10.5194/acp-18-247-2018, 2018.

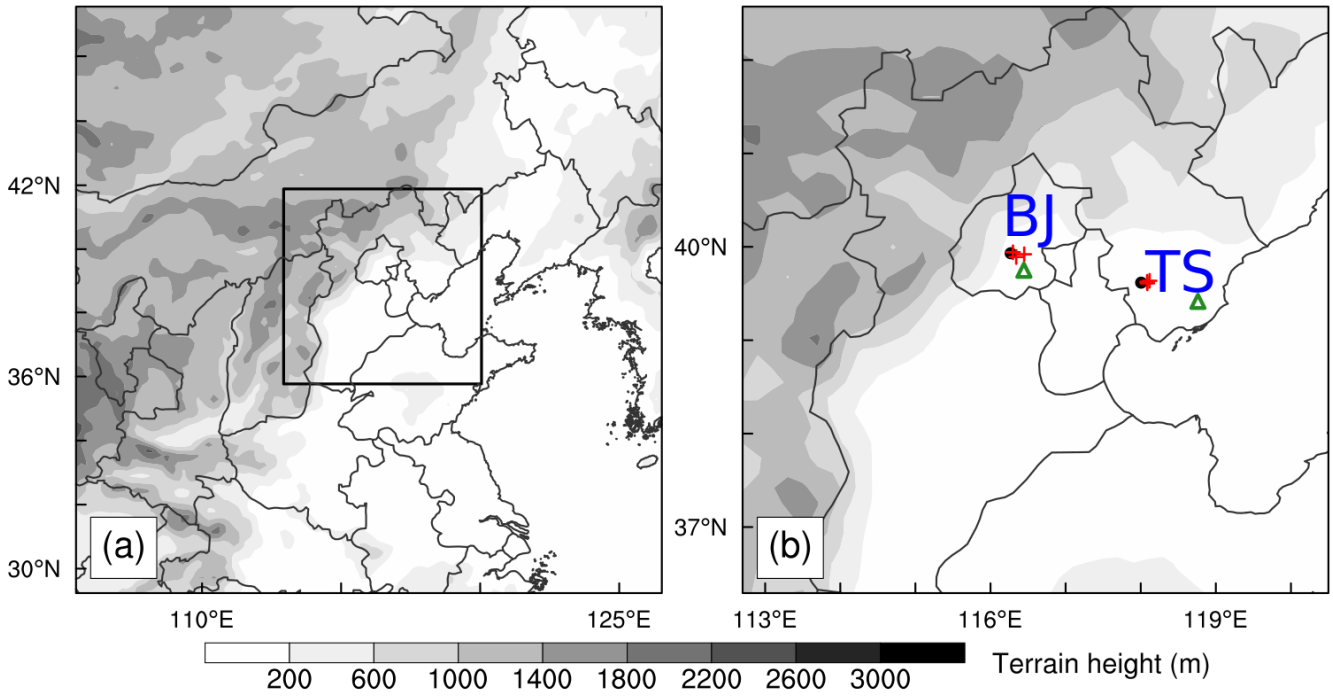

Figure 1: Maps of terrain height in (a) the simulation ~~outer~~ domain, and the approximate locations of the Beijing-Tianjin-Hebei (BTH) region is denoted by the black rectangle ~~and (b) the inner domain~~. In Fig. 1b, the locations of surface meteorological stations and air quality monitoring stations in Beijing (BJ), ~~Langfang (LF), Tianjin (TJ)~~ and Tangshan (TS) are marked by the black dots and the red crosses, respectively. The sounding sites are denoted by the green triangles.

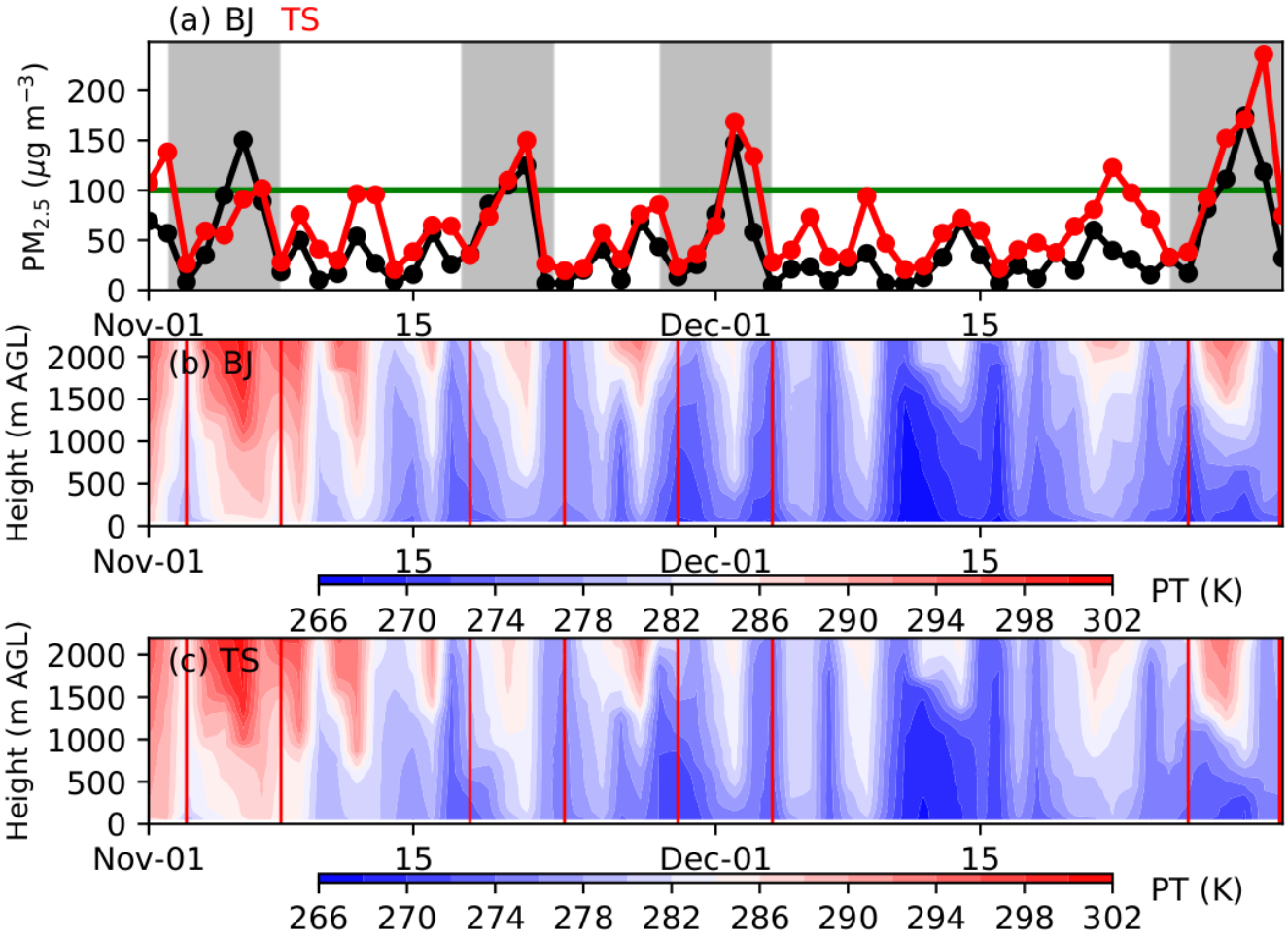

Figure 2: Time series of observed $PM_{2.5}$ concentration from 1 November to 31 December in 2017 in (a) Beijing and Tangshan~~Langfang~~, and (b, c) ~~Tianjin and Tangshan.~~ vertical structure of potential temperature (PT) derived from the sounding data at 2000 BJT ~~in (b) Beijing and (d) Tangshan~~. Four~~ive~~ heavy pollution episodes with maximum daily $PM_{2.5}$ concentration greater than 100 μg m^{-3} in both Beijing and Tangshan are marked by the~~associated with strong thermal inversions are marked by the~~ grey shadings in Fig. 2a.

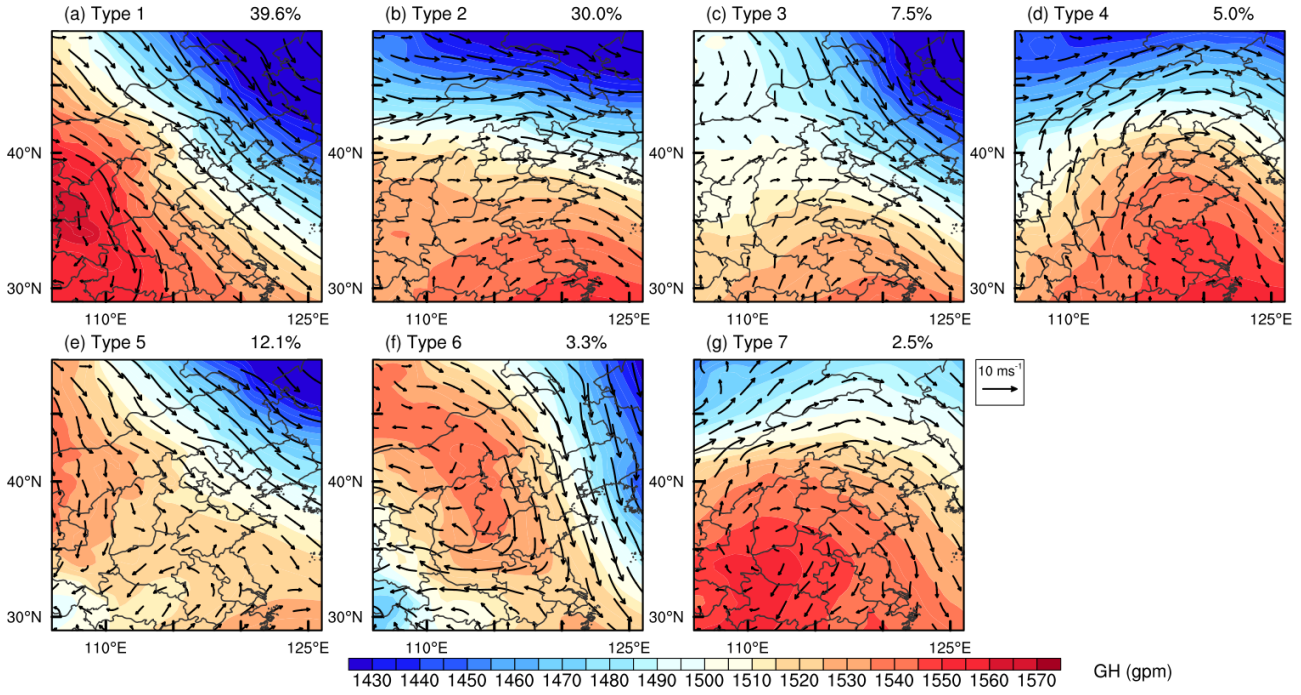

Figure 3: The 850-hPa geopotential height (GH) fields and wind vector fields for the seven classified patterns. The occurrence frequency of each synoptic pattern is~~are~~ also given.

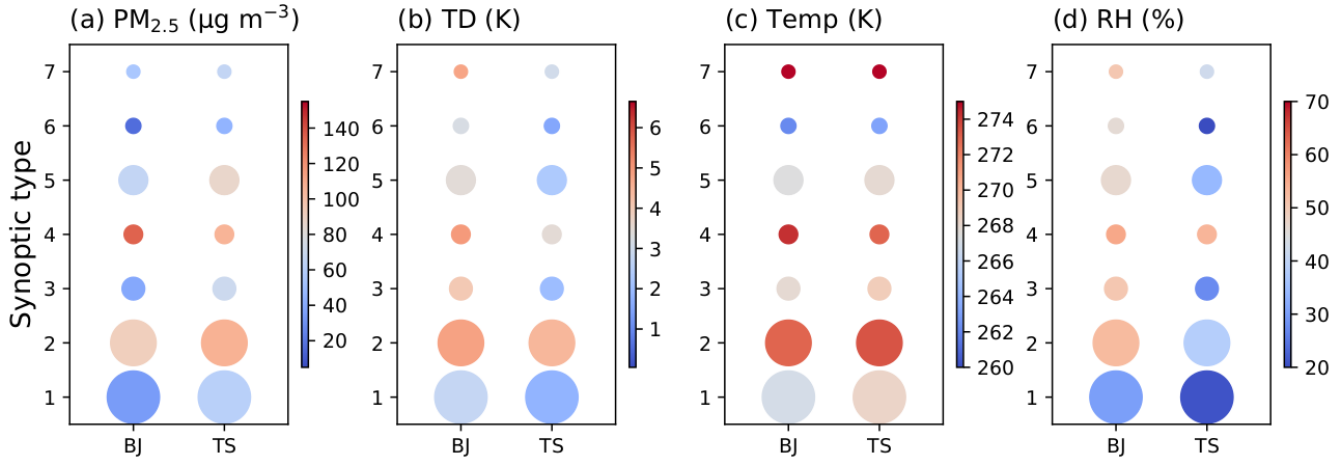

Figure 4: (a) Average ~~d~~ $PM_{2.5}$ concentrations under different synoptic conditions in Beijing~~, Langfang, Tianjin~~ and Tangshan, and ~~(b)~~ associated (b) thermal differences (TD) of PT between 100 m and 1000 m, and (c) temperature at 1000 m, and (d) relative humidity (RH) at 200 m ~~AGL in Beijing and Tangshan~~. The TD equals PT at 1000 m minus PT at 100 m. The size of circle represents the occurrence frequency of each synoptic type. All the meteorological variables shown are derived from the radiosonde data.

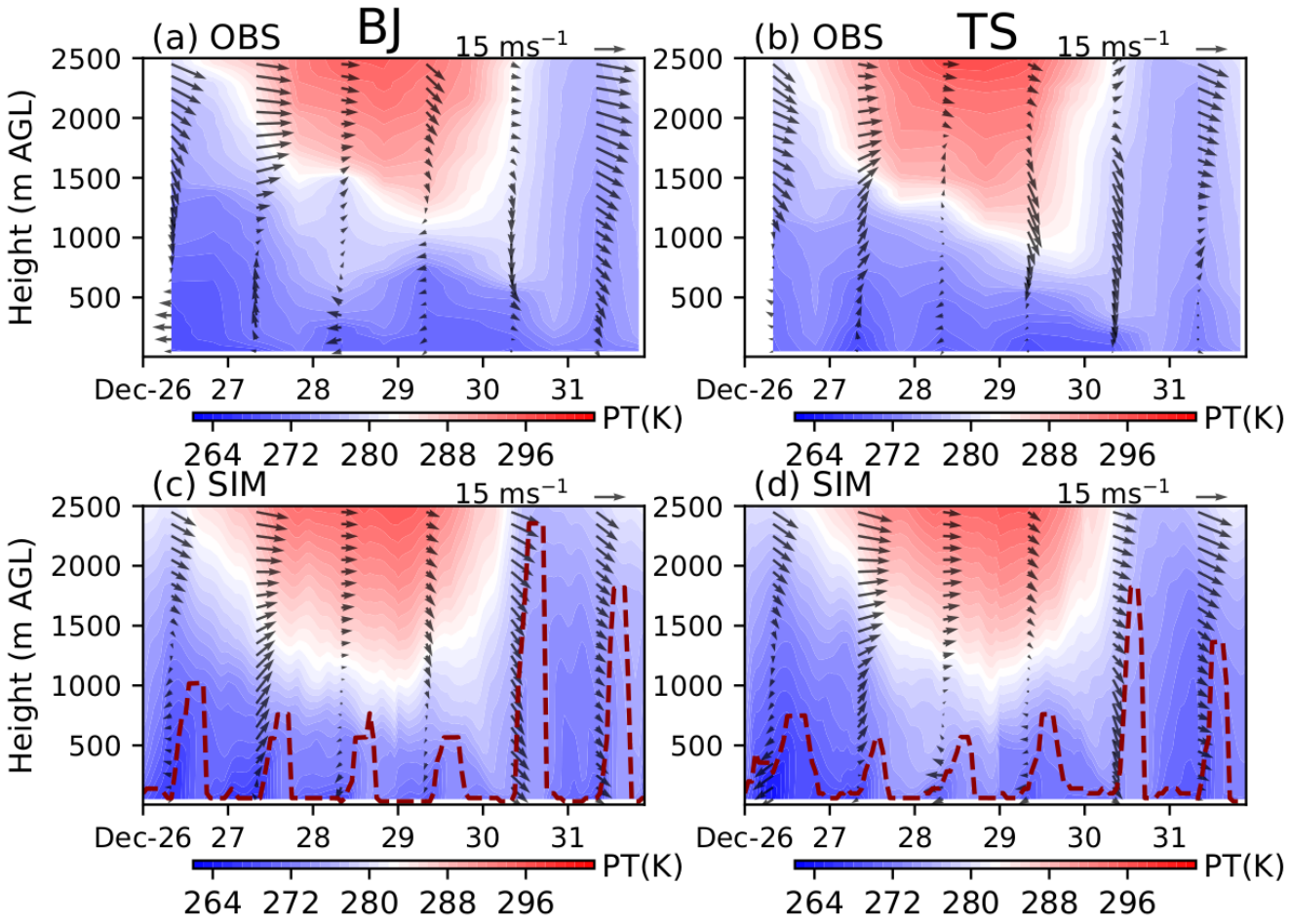

**Figure 5: Vertical structure of (a, b) observed and (c, d) simulated PT and horizontal winds in ~~(a)~~ Beijing and ~~(b)~~ Tangshan ~~during the EP1 (November 30 to December 5) and the~~ from~~EP2 (December~~ 26 to 31 December 2017~~)~~. The simulated~~PT~~ profiles are~~were~~ derived from the BASE run, and~~simulations of the grids nearest to the sounding sites. t~~The boundary layer height (BLH) is denoted by the red dash lines in Fig. 5c-d.

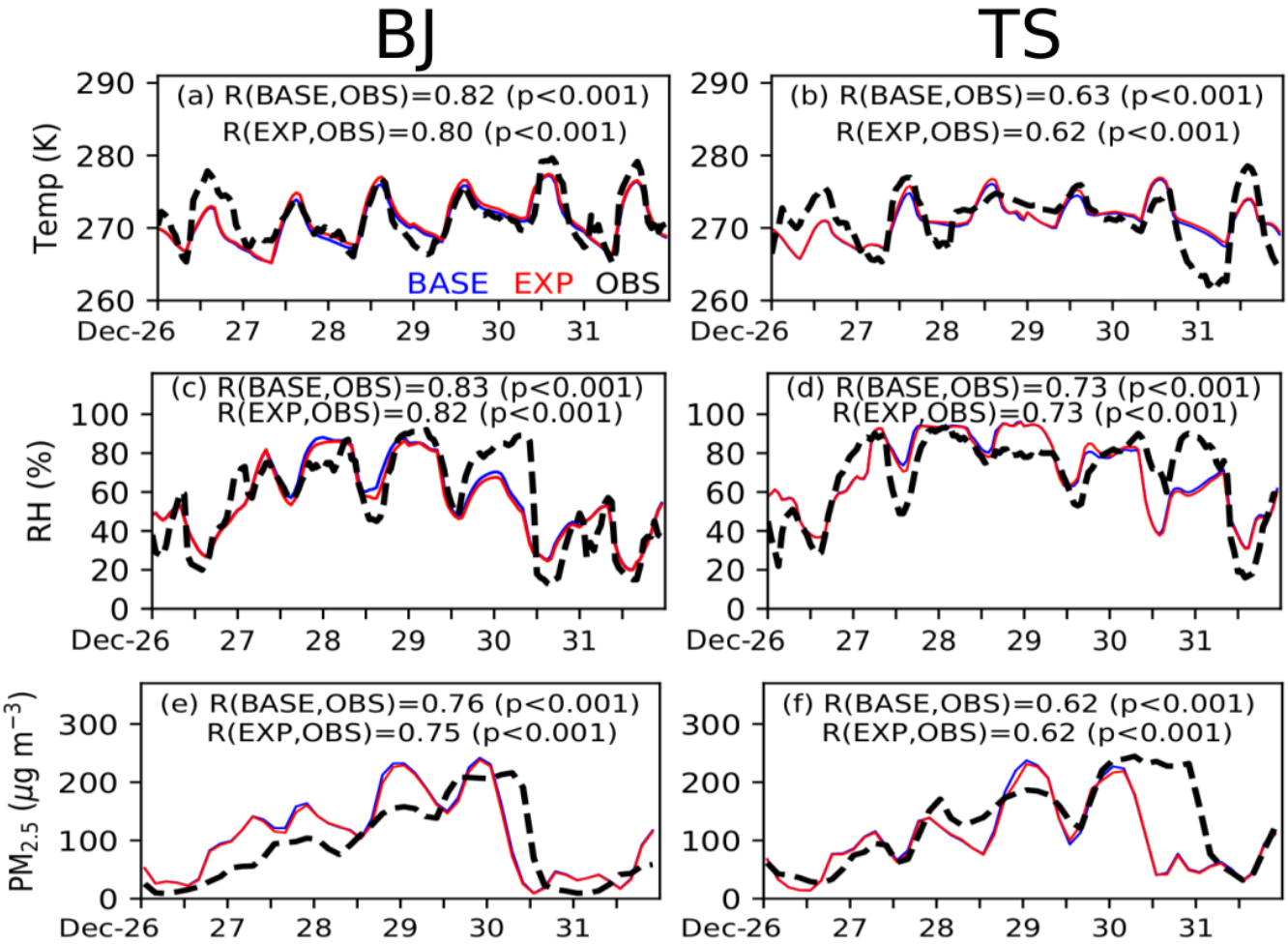

Figure 6: Time series of observed ~~(in red)~~ and simulated (a, b~~in blue~~) 2 -m temperature ~~(T)~~, (c, d) 2 -m ~~relative humidity (~~RH~~)~~, and (e, f) $PM_{2.5}$ concentration in ~~(top to bottom)~~ (left) Beijing~~, Langfang, Tianjin~~ and (right) Tangshan- from 26 to 31 December 2017~~during the EP1 and EP2~~. The simulations of BASE run are denoted in blue lines, and those of EXP run are denoted in red lines. The correlation coefficients (R) between the observations and simulations are also given for each panel.

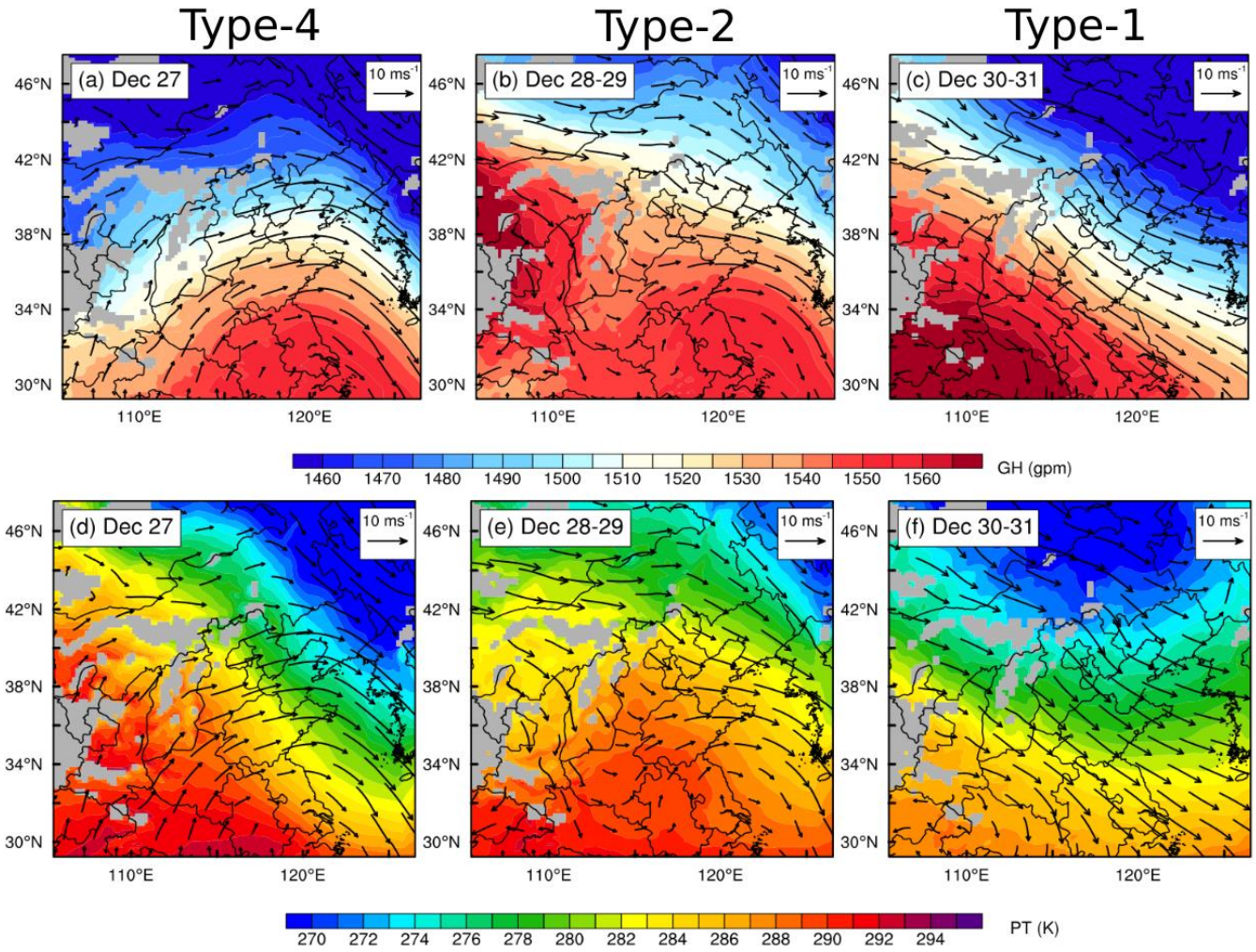

Figure 7: Simulated~~Averaged~~ **850-hPa (a-c, ~~b~~) GH and (~~c,~~ d-f) PT fields ~~during (left)~~on December 27, 28-29 and 30-31~~ 1-2~~, overlaid with the wind vectors. The regions with terrains higher than the 850-hPa level are marked by the grey shadings.~~ and (right) December 3-4, overlaid with the wind vector fields. The black line across the BTH indicates the locations of cross section shown in Fig. 8.~~

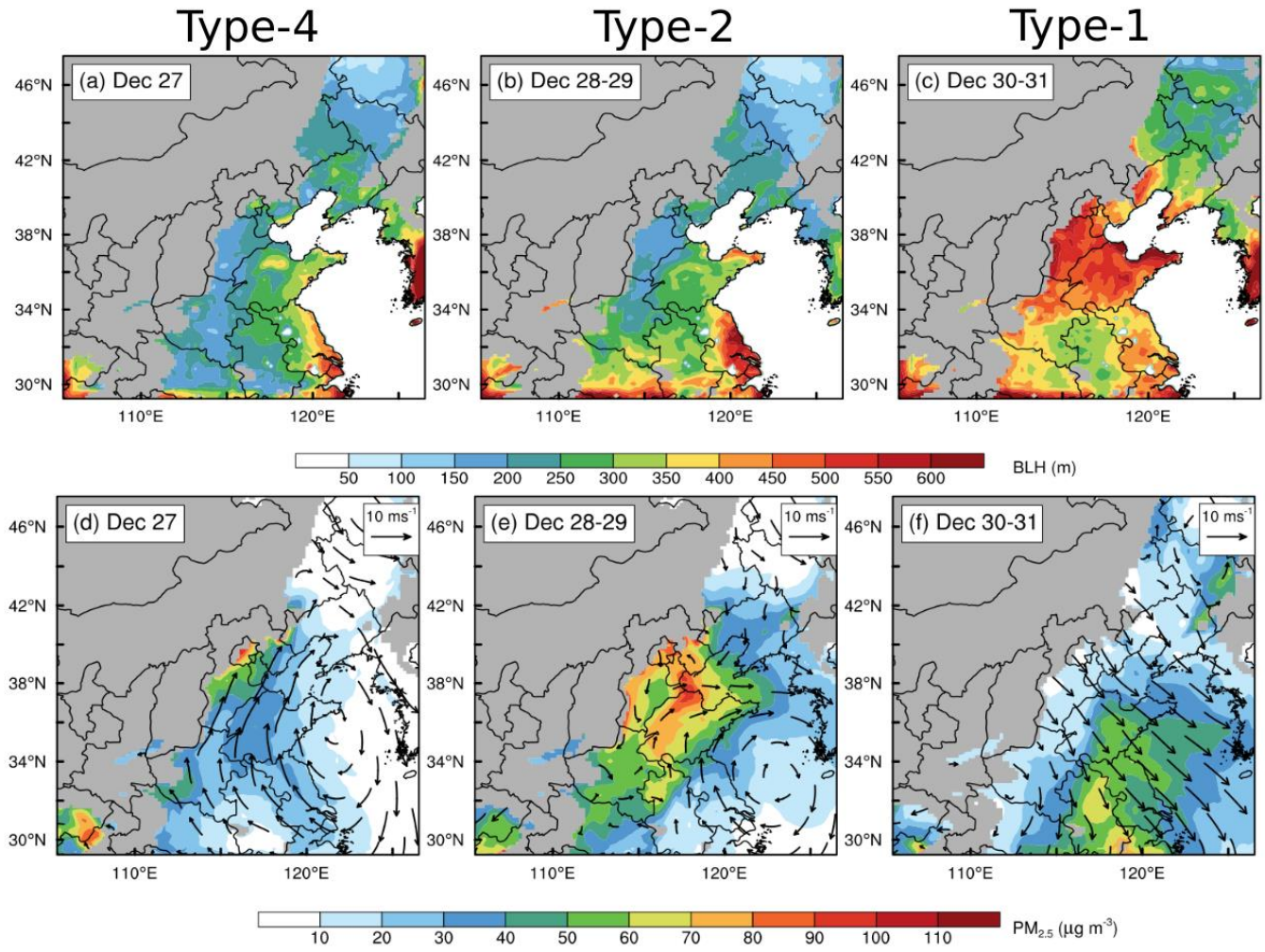

Figure 8: Spatial patterns of simulated (a-c) BLH and (d-f) 900-hPa $PM_{2.5}$ concentration and wind vectors in the plains of BTH from 27 to 31 December, 2017. The mountainous regions are denoted by the grey shadings. ~~Vertical cross sections of simulated (a, b) PT, (c, d) $PM_{2.5}$ concentration during (left) December 1-2, and (right) December 3-4. The locations of cross section (~39.5 °N) are indicated by the black line in Fig. 7. The BLH is denoted by the red line for each panel. Note that the vertical velocity is multiplied by a factor of 10 when plotting the wind vectors.~~

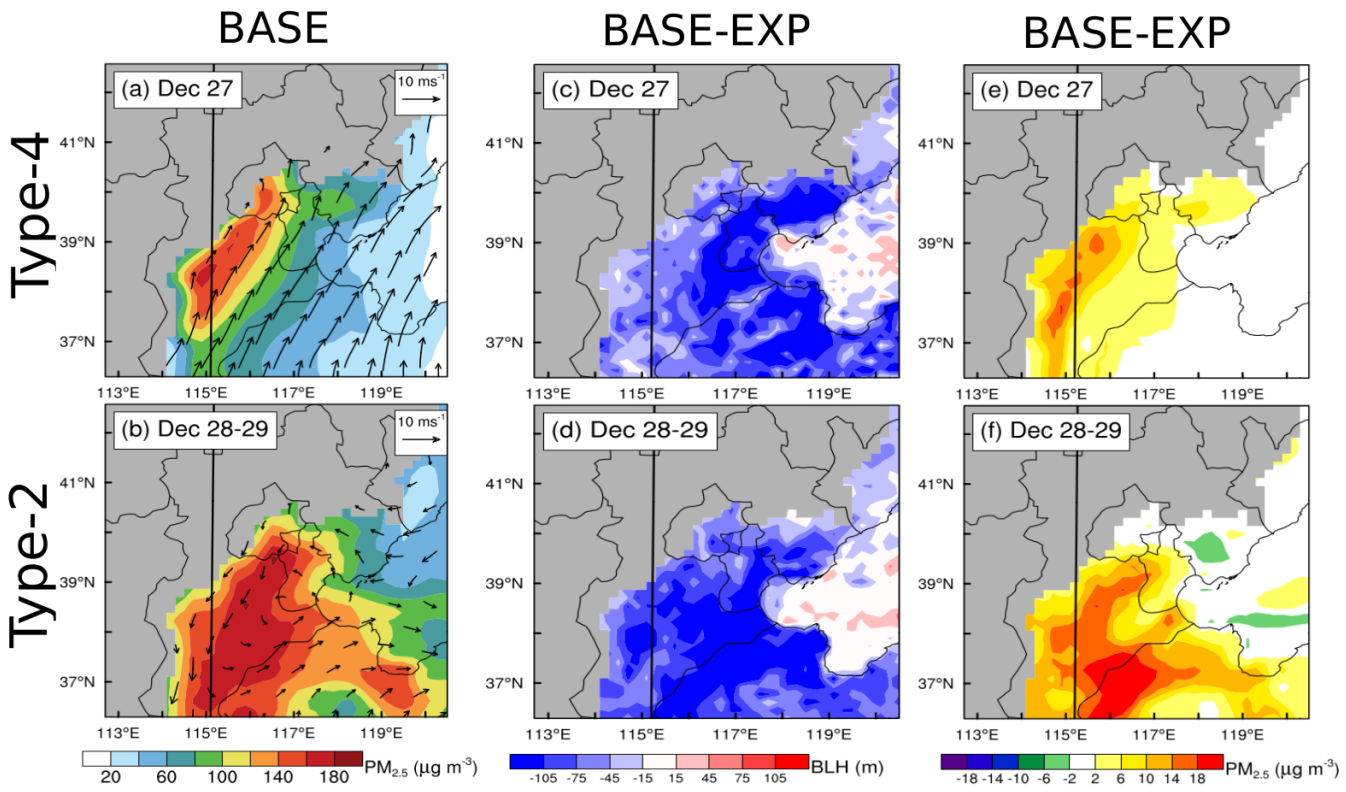

Figure 9: Spatial distribution of simulated (a, b) near-surface~~averaged (a, b) BLH and (c, d)~~ $PM_{2.5}$ concentration and wind, and the perturbations induced by the aerosol radiative effect on (c, d) BLH and (e, f) $PM_{2.5}$ in the plains of BTH during 0900 to 1600 BJT on~~during~~ (top~~left~~) December 271~~-2~~ and (bottom)~~, and (right)~~ December 283~~-294~~. The black lines in Fig. 9a indicates the locations of vertical sections shown in Fig. 10.

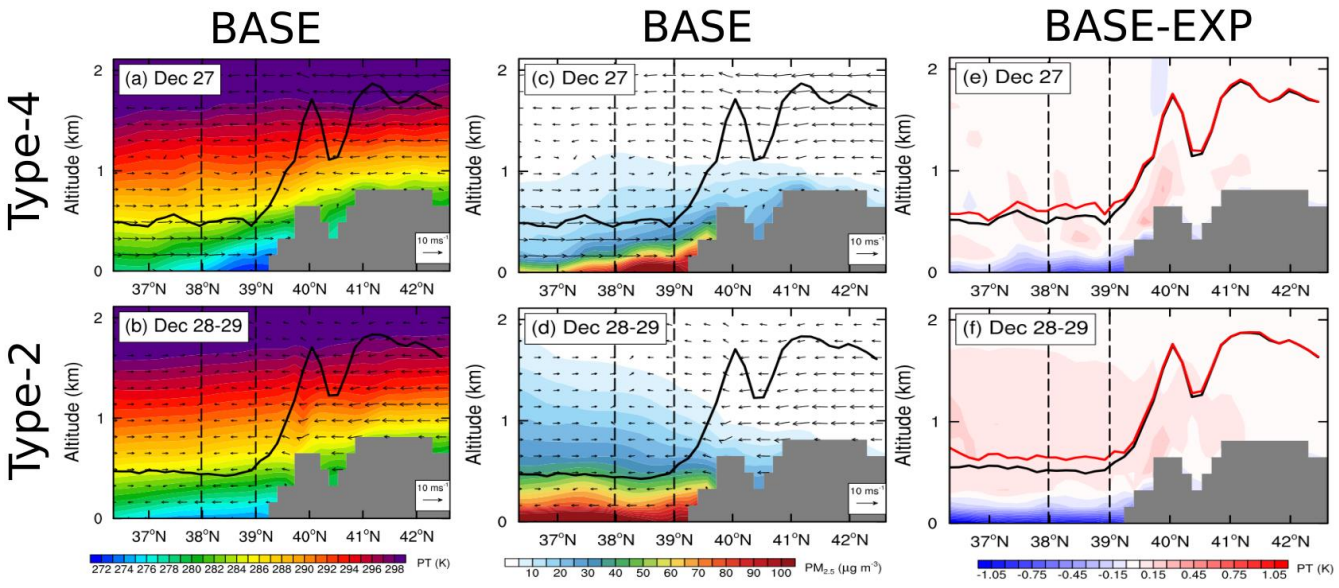

Figure 10: Vertical cross sections of ~~s~~simulated (a, b~~top~~) PT, (c, d) $PM_{2.5}$ concentration, and (e, f) the concentration perturbation induced by the aerosol radiative effect during 0900 to 1600 BJT on (top) December 27, and (bottom) December 28-29. The locations of cross section are indicated by the black lines in Fig. 9. In Fig. 10e-f, the BLH of BASE run is denoted by the black lines, and the BLH of EXP run is denoted by the red lines. Note that the vertical velocity is multiplied by a factor of 10 when plotting the wind vectors. The vertical dashed lines indicate the regions to derive the profiles of PT and $PM_{2.5}$ concentration shown in Fig. 11.~~850 hPa GH and wind fields, and (bottom) near-surface $PM_{2.5}$ concentration overlaid with 900 hPa wind fields during December 28-31.~~

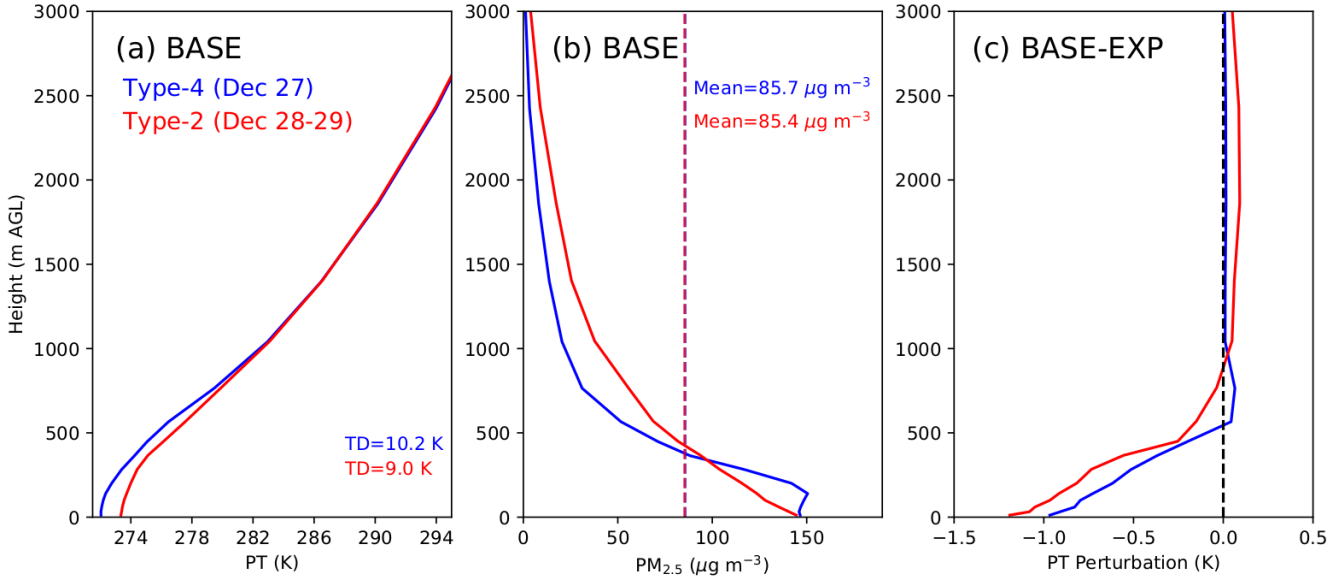

Figure 11: Average vertical profiles of simulated (a) PT, (b) $PM_{2.5}$ concentration, and (c) PT perturbations induced by the aerosol radiative effect during 0900 to 1600 BJT on December 27 (in blue) and December 28-29 (in red)~~Perturbations induced by the aerosol radiative effect on (a) BLH and (b) near-surface $PM_{2.5}$ concentration during 0800 to 1800 BJT on December 1-2. The perturbations are estimated as the differences between the BASE and EXP simulations. The black square outlines the region of interest (ROI) for the vertical profiles of $PM_{2.5}$ and PT shown in Fig. 12~~, derived from the simulations along the cross section shown in Fig. 10 between

38 °N and 39 °N. In Fig. 11a, the TD is calculated as the PT difference between 100 m and 1000 m. In Fig. 11b, the dash lines indicate the mean $PM_{2.5}$ concentrations below 3000 m AGL on December 27 (in blue) and December 28-29 (in red).

490

~~**Figure 12: (a) Time series of BLH in the ROI on December 1-2, derived from the BASE (in blue) and EXP (in red) simulations. Perturbations induced by the aerosol radiative effect on the vertical profile of (b) $PM_{2.5}$ and (c) PT in the ROI.**~~